Top Organomet Chem (2010) 28: 75–111
DOI: 10.1007/978-3-642-01866-4_3

Luminescent Platinum Compounds: From Molecules to OLEDs

Lisa Murphy and J. A. Gareth Williams

Abstract Around 30 years ago, much of the research into platinum coordination chemistry was being driven either by research into one-dimensional, electrically conducting molecular materials exploiting the stacking interactions of planar complexes, or by the unprecedented success of *cis*-$Pt(NH_3)_2Cl_2$ (cisplatin) as an anticancer agent. At that time, a number of simple platinum(II) compounds were known to be photoluminescent at low temperature or in the solid state, but almost none in fluid solution at room temperature. Since that time, several families of complexes have been discovered that are brightly luminescent, and a number of investigations have shed light on the factors that govern the luminescence efficiencies of Pt(II) complexes. Over the past decade, such studies have been spurred on by the potential application of triplet-emitting metal complexes as phosphors in organic light-emitting devices (OLEDs), where their ability to trap otherwise wasted triplet states can lead to large gains in efficiency. In this contribution, we take a chemist's perspective of the field, overviewing in the first instance the factors that need to be taken into account in the rational design of highly luminescent platinum(II) complexes, and the background to their use in OLEDs. We then consider in more detail the properties of some individual classes, highlighting work from the past 3 years, and including selected examples of their utility in OLEDs and other applications.

Keywords Electroluminescence, Luminescence, OLEDs, Photochemistry, Platinum

Contents

L. Murphy and J.A. Gareth Williams (✉)
Department of Chemistry, University of Durham, Durham, DH1 3LE, UK
e-mail: j.a.g.williams@durham.ac.uk

1 Fluorescence and Phosphorescence: Singlets and Triplets

It was Alexandre-Edmond Becquerel, in his 1867 treatise *La Lumière, ses causes et ses effets*, who first put forward a systematic distinction between fluorescence and phosphorescence. Becquerel designed a phosphoroscope that allowed precise time intervals to elapse between the exposure of a material to light and the observation of the light emitted. He defined fluorescence as emission of light that is immediately extinguished upon removal of the light source, whilst phosphorescence persists for some time after exposure.

The modern and more rigorous distinction is based in quantum theory. Fluorescence is the emission of light that occurs as the result of a spin-allowed electronic transition ($\Delta S = 0$), for example, from the first excited singlet state of an aromatic molecule to the ground state, $S_1 \rightarrow S_0$ [1]. It is normally characterised by a high radiative rate constant k_r^S of the order of 10^8–10^9 s^{-1}, leading to short emission lifetimes in the nanosecond range. Phosphorescence arises from spin-forbidden transitions ($\Delta S \neq 0$), for example, from the first excited triplet state to the ground state, $T_1 \rightarrow S_0$. In this case, radiative rate constants k_r^T are frequently small, around 1 s^{-1} for molecules such as anthracene, leading to natural lifetimes of the order of 1 s [2]. In fact, the phosphorescent process is so slow that faster processes of non-radiative decay of the triplet state normally predominate for such molecules in solution at room temperature, so that phosphorescence is not observed. Only by cooling the sample down to low temperatures and rigidifying it to inhibit such processes is the phosphorescent light observable. The key radiative and non-radiative processes involved are typically represented by a Jabłonski diagram; an example for an organic compound is given in Fig. 1.

In the case of photoluminescence, where the molecule is excited by light, the proportion of triplet and singlet states formed depends upon the relative magnitudes of

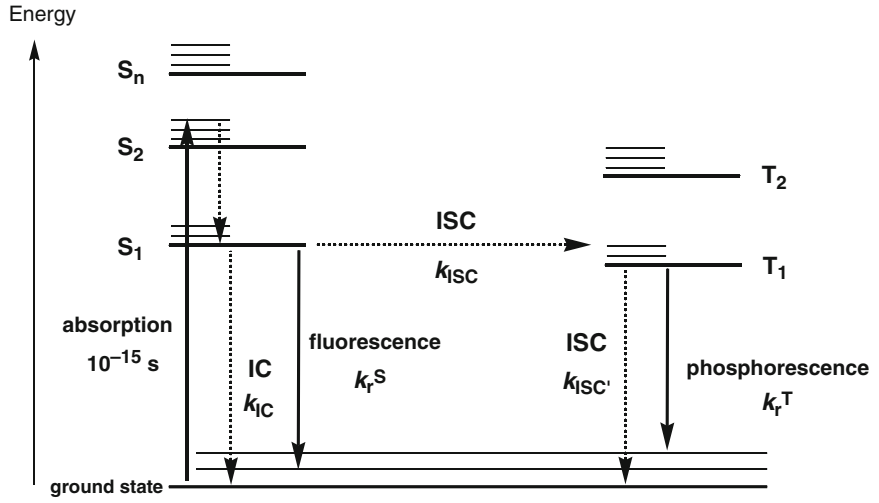

Fig. 1 A simplified Jabłonski diagram for a conjugated organic molecule such as anthracene, illustrating the rate constants for key processes as defined in the text. 'IC' represents internal conversion (an isoenergetic process) followed by vibrational relaxation; similarly 'ISC' represents intersystem crossing followed by vibrational relaxation

k_r^S and k_{ISC}, where k_{ISC} is the rate constant for intersystem crossing from S_1 to T_1. For simple conjugated molecules like naphthalene, anthracene and pyrene, these two parameters have similar values to one another, leading to fluorescence quantum yields of the order of 0.5. In contrast, in cases such as benzophenone, where the difference in energy between S_1 and T_1 is very small, k_{ISC} may be very high such that no significant fluorescence is observed, and the efficiency of triplet formation approaches unity.

Irrespective of the triplet yield, once formed, the radiative rate constant of the triplet state is normally low. If a heavy atom – such as a third row transition metal ion – is brought close to the π-system of the molecule, in such a way that there is significant mixing of the orbitals, then k_r^T can be greatly increased, sometimes by up to 10^6 or more, due to the large spin–orbit coupling associated with the heavy atom which scales with Z^4. Radiative emission can now compete with deactivating processes allowing phosphorescence to be observed at room temperature.

2 Electroluminescence and OLEDs

Organic light-emitting devices (OLEDs) are based on electroluminescence. The energy required to raise the emitting molecule to the excited state is supplied electrically, rather than by the absorption of higher-energy light as it is in photoluminescence. Briefly, a thin layer of the emissive material is sandwiched between two electrodes [3]. Upon application of the electric field, the material is reduced

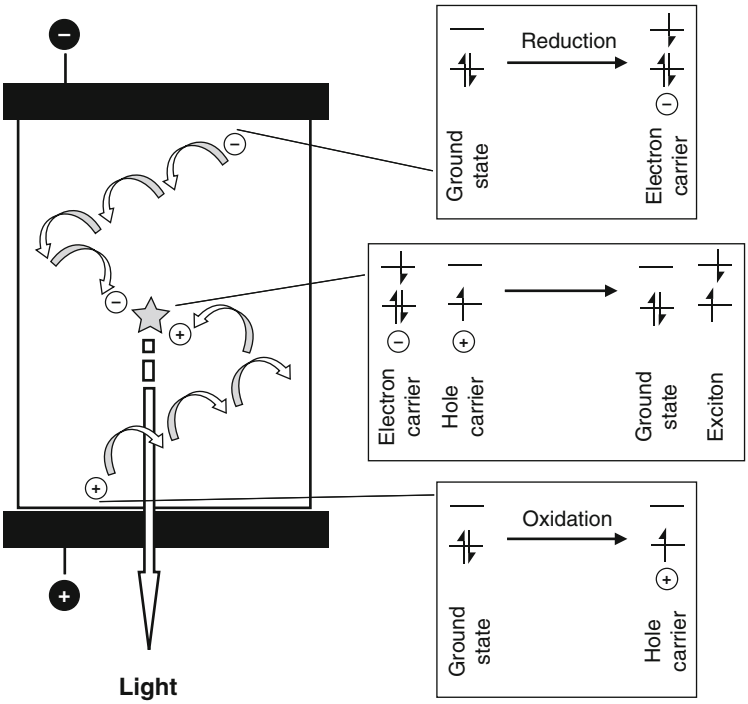

Fig. 2 Schematic representation of electroluminescence in organic materials

at the cathode and oxidised at the anode to give electron and hole carriers, respectively, which migrate under the applied field towards the other electrode. When two such charge carriers of opposite sign meet, they combine to produce one molecule in the ground state and one in the excited state (Fig. 2). In contrast to photoluminescence, both singlet and triplet excited states (also known as excitons) are now formed *directly*, and their proportion is governed primarily by the statistics of charge recombination, leading to a theoretical 1:3 (S:T) ratio [4]. In a purely organic light-emitting device, emission from the triplet states is forbidden, so the efficiency is capped at 25%. This represents a huge wastage of energy, which simply goes into heating up the device.

As noted in Sect. 1, the introduction of a heavy metal ion onto a conjugated organic molecule can greatly accelerate the S ← T process through the influence of spin–orbit coupling. Thus, by incorporating such phosphorescent materials into the emissive layer of the device, emission from the triplet excitons can be promoted, and quantum efficiencies of 100% potentially achieved.

The first metal-based phosphorescent dopant to be investigated as such a 'triplet-harvesting' dopant in an OLED was platinum(II) octaethylporphyrin, **1** [5]. Upon doping this compound into the widely-used EL emissive material Alq_3 {tris(8-quinolinato)aluminium, **2**}, 90% of the energy is transferred from the host to the porphyrin, and a device of internal electroluminescence efficiency of 23% (external

EL = 4%) obtained [6]. Given that the triplets are now clearly emitting too, why isn't the device efficiency higher? Part of the reason is the long phosphorescence lifetime of **1** (~80 μs in solution), which results in severe triplet-triplet annihilation, particularly at high current (Eq. 1); in other words, the triplet excited state is so long-lived that it survives long enough to encounter other triplet excitons, and half the energy is lost non-radiatively. Clearly, there is a need for new complexes that emit efficiently but with shorter radiative lifetimes. Ways of achieving this are addressed in the following section.

$$4(^3M^* + {}^3M^*) \rightarrow {}^1M^* + 3^3M^* + 4M. \quad (1)$$

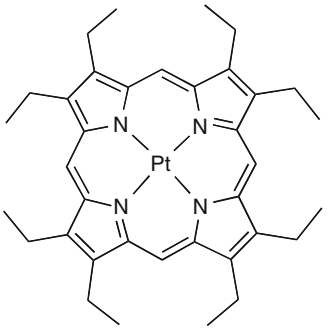

1

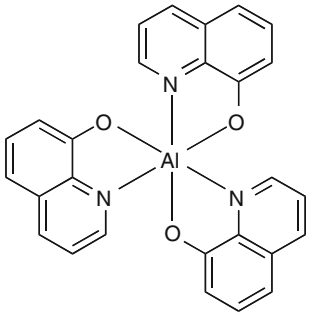

2

3 Designing Highly Luminescent Platinum Complexes

In common with fluorescent molecules, the efficiency of luminescence of metal complexes from triplet excited states, η_r^T, will be favoured by high radiative rate constants k_r^T and low rate constants for non-radiative decay pathways $\sum k_r^T$:

$$\eta_r^T = k_r^T / \left\{ k_r^T + \sum k_{nr}^T \right\}. \quad (2)$$

In photoluminescence, the observed triplet luminescence quantum yield, Φ_{lum}^T, also depends on the efficiency of formation of the triplet state upon absorption of light, in turn determined by the magnitude of the rate constant of intersystem crossing, k_{ISC} (Eq. 3), where k_r^S and $\sum k_{nr}^S$ are the radiative and non-radiative decay rate constants of the singlet state:

$$\Phi_{lum}^T = \eta_r^T \cdot k_{ISC} / \left\{ k_r^S + \sum k_{nr}^S \right\}. \quad (3)$$

The high spin–orbit coupling constant of the platinum nucleus ($\chi = 4{,}481\ \mathrm{cm}^{-1}$) should facilitate both the S → T intersystem crossing process and the T → S radiative decay. However, the extent to which it does so in a complex will depend upon the contribution of metal atomic orbitals to the excited state. In many simple Pt(II) complexes with relatively small ligands, the metal's involvement is such that triplet state formation is very fast, of the order of $10^{12}\ \mathrm{s}^{-1}$ [7]. Since this greatly exceeds typical singlet radiative rate constants of aromatic ligands, emission is then

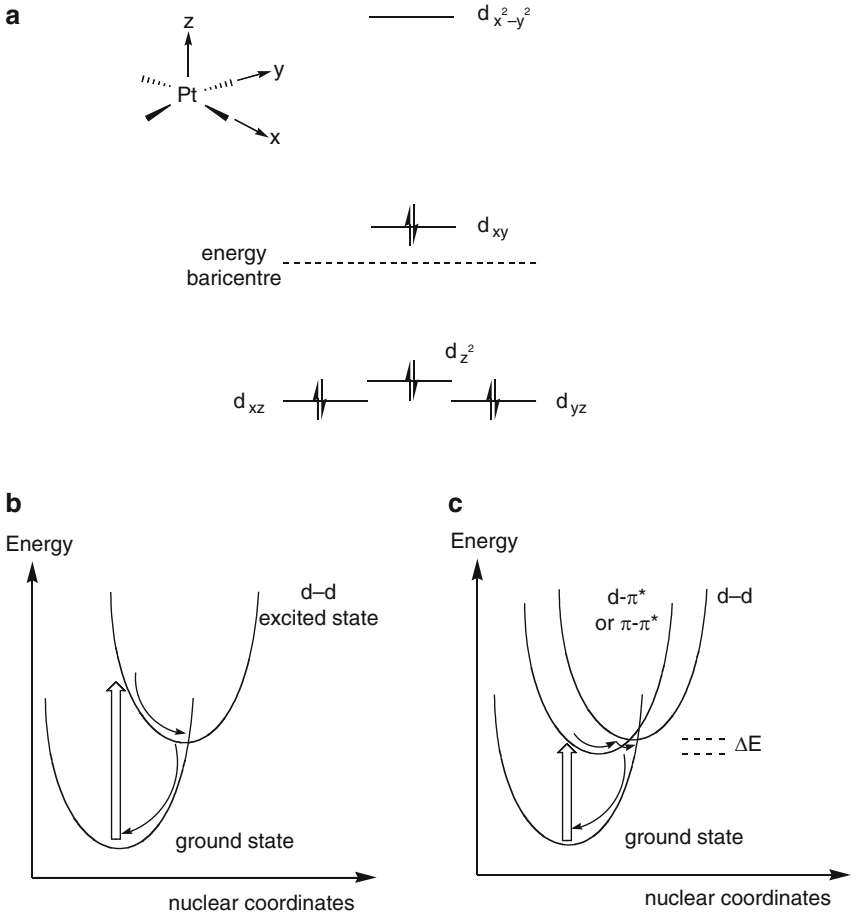

Fig. 3 (**a**) Simple ligand field splitting diagram for metal *d* orbitals in a square planar d^8 complex. The *z* axis is, by convention, perpendicular to the plane of the complex and the M–L bonds lie along the *x* and *y* axes. Although the ordering of the lower energy levels depends on the ligand set (e.g. relative importance of σ- and π-effects), the d_{x2-y2} is always the highest. (**b**) The displaced potential energy surface of the *d–d* excited state formed by population of the d_{x2-y2} orbital. (**c**) The *d–d* state can provide a thermally activated decay pathway for other, lower-lying excited states if ΔE is comparable to kT. *Thick arrows* represent absorption of light; *thin ones* indicate vibrational relaxation and non-radiative decay

observed exclusively from the triplet states. On the other hand, if the excited state is localised on a remote part of a more extended ligand, well removed from the metal centre, or if the pertinent orbitals are orthogonal and hence poorly mixed, ligand-based singlet fluorescence may be observed [8, 9].

Similarly, the radiative rate constant k_r^T is likely to be larger for excited states in which the metal plays a significant role; e.g. MLCT states, or LC states that are significantly perturbed by the metal [10].

Equally important is the need to minimise the rate of non-radiative decay, Σk_{nr}. In the case of square planar platinum(II) complexes, this is often determined primarily by the energy of metal-centred (*d–d*) states, a point that can be readily understood in terms of the ligand-field splitting diagram of square planar d^8 complexes (Fig. 3a) [11]. The unoccupied d_{x2-y2} orbital is strongly antibonding. Population of this orbital will therefore be accompanied by elongation of Pt–L bonds and severe distortion, which promotes non-radiative decay to the ground state due to the isoenergetic crossing point lying at accessible energies (Fig. 3b). Of course, in many platinum(II) complexes, LC and MLCT states may lie lower in energy than these *d–d* states, but the latter will still exert a deleterious influence if they are thermally accessible, i.e. if ΔE is comparable to kT (Fig. 3c). Let us take an example. In the simple bipyridyl complex Pt(bpy)Cl_2 **3**, the *d–d* state is the lowest-lying excited state, and the complex does not emit at room temperature [12]. In the analogous complex of the ester-substituted bipyridine, Pt{3,3'-$(MeCO_2)_2$-bpy}Cl_2 **4**, the lowest-lying excited state is now the MLCT state, but the *d–d* state lies only a little higher in energy, offering the former a non-radiative decay pathway and also rendering this complex non-emissive at room temperature [13].

3.1 Tuning Excited States to Optimise Luminescence Efficiencies

The above discussion leads naturally to the conclusion that the most emissive platinum(II) complexes will be those in which (1) the lowest-energy excited state is *not* a metal-centred *d–d* state but rather an LC or CT state, and (2) where the energy gap between the lowest excited state and the *d–d* state is sufficiently large as to prevent thermally activated decay via the latter.

For example, platinum(II) porphyrins are perhaps the oldest known class of luminescent Pt(II) complexes. They emit deep into the red region (e.g. $\lambda_{max} =$ 641 nm, $\Phi_{lum} = 0.6$ for **1** [14]). Clearly the emissive, porphyrin-based π–π* state is sufficiently low in energy that activation to the *d–d* state is ruled out at room temperature. However, relying on the low-energy of the emissive state to disfavour non-radiative decay is clearly not an option if higher-energy blue- or green-emitting complexes are sought! In such cases, it is necessary to work on ensuring that the *d–d* states in the complex are kept at high energies [11]. In practice, this means that strong-field ligands need to be present in the coordination sphere of the metal ion.

For example, in contrast to $Pt(bpy)Cl_2$ mentioned above, complexes of the form $Pt(bpy)(–C{\equiv}C–Ar)_2$ are normally quite strongly emissive in solution at room temperature [15]. The difference can be attributed – at least in part – to the stronger ligand-field associated with the acetylide compared to the chloride co-ligands. Similarly, cyclometallated ligands, particularly those offering the metal ion a synergistic combination of a π-accepting heterocycle (e.g. pyridine) with the strongly σ-donating cyclometallated carbon, lead to a strong ligand field. This accounts, for example, for $[Pt(N^C\text{-}ppy)(N^N\text{-}bpy)]^+$ being luminescent at room temperature, in contrast to $[Pt(N^N\text{-}bpy)_2]^{2+}$, which is not (ppyH = 2-phenylpyridine) [16]. A more comprehensive discussion of these principles is provided in a recent contribution to the sister volume of this series [11].

In this chapter, we shall overview some of the main classes of platinum(II) complexes that are luminescent under ambient conditions, highlighting those which have been shown to be potentially useful OLED dopants [17]. The emphasis is on examples from the past 3 years, although naturally not to the exclusion of important and informative earlier original examples.

4 PtL_2X_2 Complexes (L = Neutral $2e^-$ Donor Ligand, X = Anionic Ligand)

Many of the complexes which fall into this class are Pt(N^N)-based compounds, where N^N is a bidentate diimine ligand such as bipyridine or phenanthroline and derivatives thereof. As noted in Sect. 3, those where X = Cl are rarely significantly emissive, because the *d-d* state is either the lowest-energy excited state or is thermally accessible from a lower-lying CT or LC state [13].

4.1 X = –C≡N

The substitution of the halides by strong-field cyanides (X = –C≡N) lowers the energy of the highest-occupied metal-centred orbitals and raises the vacant d_{x2-y2} orbital, such that $Pt(N^N)(CN)_2$ complexes normally emit from π–π* states. Many of these complexes also form emissive excimers [18–20]. For example, $Pt(dpphen)(CN)_2$ **5** displays green emission centred at 520 nm in dilute CH_2Cl_2 (10^{-5} M), but increasing the concentration leads to the appearance of a red emission band, centred at 615 nm, which grows in at the expense of the green band with an identical excitation spectrum [19]. The red emission is attributed to an excimer analogous to well-known examples amongst planar organic compounds such as pyrene, and formed from the bimolecular interaction of an excited monomer with a ground-state monomer [21].

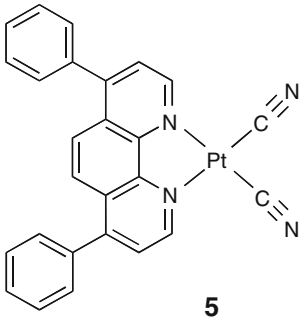

5

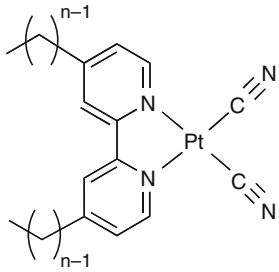

6

Very recently, Kato and colleagues prepared Pt(dC$_n$bpy)(CN)$_2$ **6** complexes bearing long alkyl chains, where dC$_n$bpy represents bipyridine substituted at the 4 and 4′ positions by –C$_9$H$_{19}$ ($n = 9$) or –C$_{11}$H$_{23}$ ($n = 11$) [22]. These compounds could be prepared by treatment of the respective ligands with platinum dicyanide in a mixture of DMF and aqueous ammonia. The long chains render the complexes soluble in a wider range of solvents than the parent systems, and to higher concentrations, which has allowed the solvent dependence of excimer formation to be investigated. In polar solvents such as methanol and acetonitrile, exclusively monomer emission is observed over the concentration range 10^{-5} to 10^{-3} M. Over the same range in chloroform, the emission switches from monomer to excimer, whilst in toluene solution, the excimer is observed even at 10^{-5} M. Evidently, the reorganisation of the molecules to form the excimer is favoured by solvents of low polarity. The difference is strikingly revealed by the change in the emission spectrum of a 5×10^{-5} M solution of the $n = 9$ complex in different ratios of $CHCl_3$/toluene (Fig. 4).

In an unusual recent development, Kunkely and Vogler have investigated the excited state properties of Pt(COT)(CN)$_2$ **7** (COT = cyclo-octatetraene) [23]. The COT ligand can be thought of as an analogue of a diimine, in that it has relatively low-energy π* orbitals. Indeed, the complex in the solid state displays a long-wavelength absorption maximum centred at 430 nm and intense orange emission at 572 nm, attributed to the singlet and triplet MLCT {Pt^{II} → π*(C$_8$H$_8$)} states respectively (Fig. 5). Unfortunately, in solution, the complex is of limited stability and degrades with release of COT.

In addition to excimer formation, square planar platinum(II) complexes are frequently able to participate in ground-state intermolecular interactions through their axial positions. In some cases, this leads to oligomerisation through overlap of the d_{z2} orbitals that are orthogonal to the plane of the complex [24, 25]. The combination of isonitriles and cyanides as ligands for Pt(II) has been extensively studied by Mann and co-workers in their work on vapochromic sensors [26, 27]. The intermolecular interactions in double salts of the type [Pt(CNR)$_4$][Pt(CN)$_4$] and the related neutral complexes [Pt(CNR)$_2$(CN)$_2$]$_2$ are influenced by the presence of volatile organic solvents, leading to characteristic changes in colour [28].

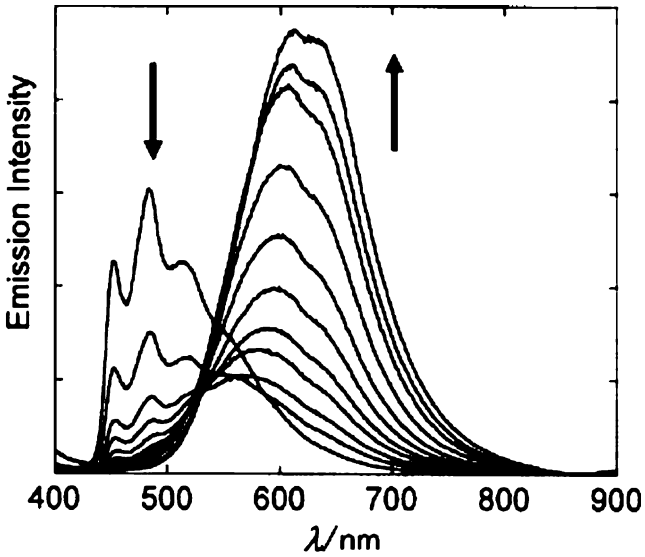

Fig. 4 Change in the emission spectrum of $[Pt(dC_9bpy)(CN)_2]$ (**6**, $n = 9$) (5×10^{-5} M; $\lambda_{ex} = 320$ nm) in different ratios of $CHCl_3$/toluene, from 100% $CHCl_3$ to 100% toluene in 10% steps [22]

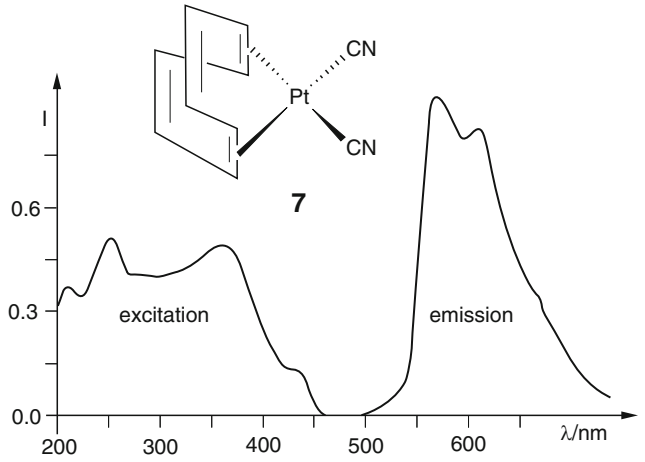

Fig. 5 Excitation ($\lambda_{em} = 572$ nm) and emission ($\lambda_{ex} = 400$ nm) spectra of solid $Pt(COT)(CN)_2$ **7** at room temperature. Reprinted from [23] with permission from Elsevier

Recently, Wang and Che have described luminescent micro- and nano-wires that form by self-assembled aggregation of $[Pt(CN^tBu)_2(CN)_2]$ directed by Pt···Pt interactions [29]. This complex itself is non-emissive in acetonitrile solution at room temperature, but displays bright green luminescence from the rod-like crystalline form. The corresponding X-ray structure reveals infinite linear stacks

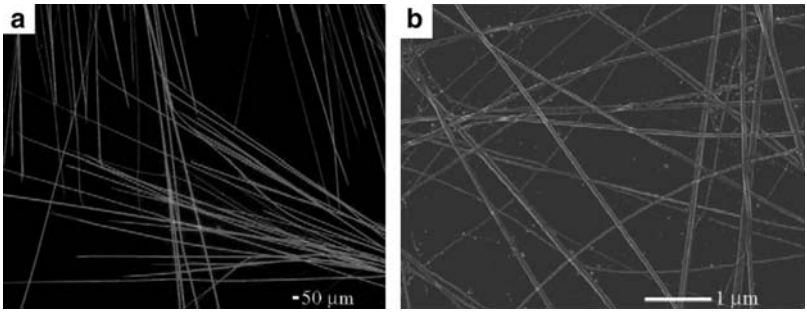

Fig. 6 (**a**) Emission microscopy image of luminescent $[Pt(CN^tBu)_2(CN)_2]$ wires formed on a silicon substrate by slowly evaporating a 10^{-4} M solution in MeCN. (**b**) Scanning electron micrograph of thinner wires of the same compound formed by injecting 50 mL of a 9.6×10^{-3} M solution in MeCN into 10 mL of water, followed by transfer onto a silicon substrate. Note the different magnification in the two images. Reprinted from [29] with permission from Wiley

comprised of pairs of complexes, with a torsion angle of 125.20° between them about the stack axis, and close Pt···Pt distances of 3.354(1) Å. Evaporation of an acetonitrile solution in air on a silicon substrate led to luminescent wires of diameter approximately 25 μm and lengths as great as 1,000 μm or more, which could be readily visualised by emission microscopy (Fig. 6a). Wires of smaller diameter could be prepared by prior dilution of the acetonitrile solution with water; an example visualised by scanning electron microscopy is shown in Fig. 6b. The luminescence emitted by the wires ($\lambda_{max} = 562$ nm at 298 K) resolves out into two components at 77 K ($\lambda_{max} = 545$ and 597 nm). The former is attributed to the dimeric Pt_2 $^3[5d\sigma^* \rightarrow 6p\sigma]$ excited state and the latter to trimeric and tetrameric species, an assignment supported by recent density functional theory (DFT) calculations [30].

4.2 X = Organometallic Carbon

Organometallic derivatives of the form Pt(N^N)(–Ar)$_2$, incorporating Pt–aryl bonds, have also been studied. They are accessible by reaction of the diimine ligands (e.g. bpy or phen) with Pt(COD)(aryl)$_2$ precursors, in turn formed from $Pt(COD)Cl_2$ and the corresponding aryl-lithium reagent [31]. The bis-mesityl complex **8** emits at 660 nm in toluene solution at room temperature from a ^{3}MLCT state [32]. Clearly, the strongly σ-donating aryl groups serve to lower the energy of the excited state. The mesityl complexes are unusual amongst square planar platinum(II) compounds in that they can be reversibly oxidised to remarkably persistent d^7 Pt(III) species, an effect attributed to the effective protection of the axial positions by the two mesityl groups [31].

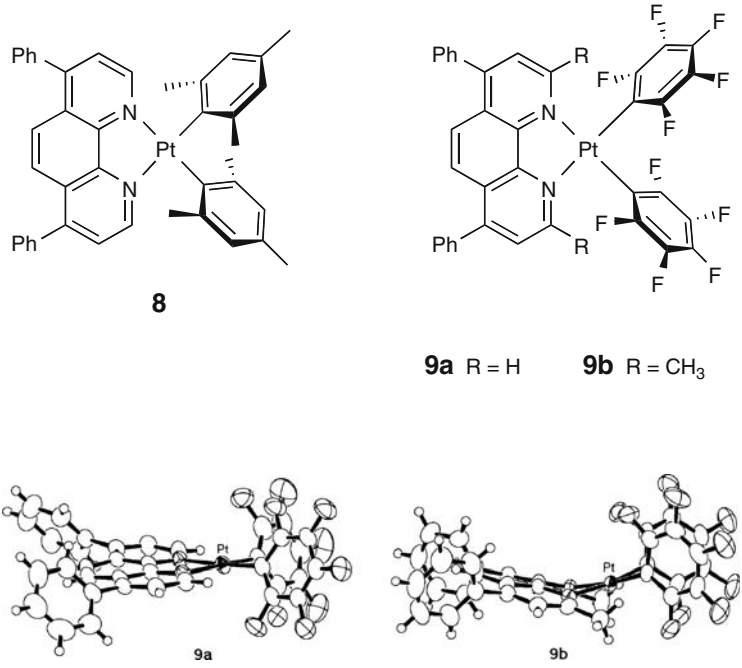

Fig. 7 Molecular structures of **9a** and **9b** in the solid state from X-ray diffraction analysis [33]

More recently, related compounds containing perfluorinated aryl rings have been prepared, e.g. **9** [33]. Like the mesityl systems, the aryl rings are twisted by about 70° with respect to the PtN_2C_2 square plane in the solid state structures (Fig. 7). The emission of Pt(dpphen)$(Ar^F)_2$ **9a** ($\lambda_{max} = 515$ nm in CH_2Cl_2) is substantially blue-shifted compared to the mesityl compound **8**, which can be readily rationalised in terms of the electron-withdrawing influence of the fluorine substituents in lowering the energy of the metal-centred HOMO. No emission could be detected from the analogous complex incorporating methyl substituents at the 2 and 9 positions of dpphen, **9b**. The X-ray structure of this complex reveals a bent structure (Fig. 7) and slightly longer Pt–N bonds owing to steric hindrance of the methyl groups, both of which features will lead to a weaker ligand field at the metal and to a less rigid structure, promoting non-radiative decay. The fluorine substituents aid sublimation, and a multi-layer OLED incorporating 6% by mass of **9a** within a CBP host emissive layer has been prepared by thermal deposition; it displays an external quantum efficiency of 2.1% at 100 cd m^{-2}.

Fekl and co-workers have recently reported the first examples of diimine-coordinated platinum complexes with 9,10-dihydroplatinaanthracene co-ligands [34]. These compounds are metallacycles: the Pt ion replaces one carbon atom within the carbocyclic system (anthracene). Reaction of the new organometallic oligomeric platinum precursor $\{[H_2C–(C_6H_4)_2]Pt(SEt_2)\}_n$ ($n = 2,3$) with diimines

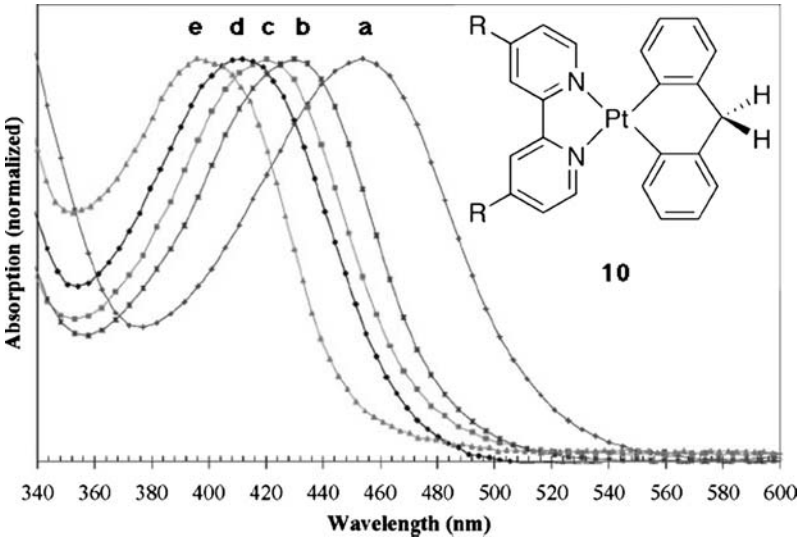

Fig. 8 Normalised charge-transfer-to-diimine absorption bands for metallacycles **10a–e** in MeCN at room temperature. Identity of R: a = Cl, b = H, c = *t*-Bu, d = MeO, e = NMe_2. Reprinted from [34] with permission from ACS

such as bipyridines, phenanthrolines and biquinoline provides easy access to a whole range of new complexes incorporating the metallacycle. The lowest-energy absorption bands of the bipyridyl series **10a–e** increase in energy as the diimine becomes more electron-rich, in line with charge-transfer-to-diimine character to the lowest spin-allowed excited state (Fig. 8). This is supported by electrochemistry and DFT calculations, which suggest that the HOMO is based primarily on the platinacycle. Although none of the compounds prepared to date display detectable emission in solution at room temperature, they emit brightly in the solid state, showing a trend in emission energies that is largely consistent with that in absorption.

4.3 L_2X_2 = Salen and Derivatives

Oxygen ligands on their own are generally not suitable for forming stable complexes with the soft Pt(II) ion, but in combination with other ligands such as diimines, complexes with high thermodynamic stability can be obtained. Shagisultanova reported that the well-known tetradentate ligand, *N*,*N*'-bis(salicylidene)-1,2-ethylenediamine or salen, forms a highly luminescent complex with Pt(II), **11** [35]. The emissive excited state is probably one of d(Pt)/π(O) → π*(Schiff base) character. Che and co-workers investigated this complex and its tetramethylethylenediamine analogue as sublimable, green-emitting OLED dopants [36]. At the

optimised dopant concentration of 4 wt%, a maximum external quantum efficiency of 11% was achieved at 8.5 mA cm^{-2}. The same team has also explored complexes of related ligands based on dpphen or tbbpy appended with ortho-phenoxy groups, which prove to be superior in terms of solution quantum yields; e.g. $\Phi = 0.6$ for **12** in DCM compared to 0.19 for **11** in MeCN [37].

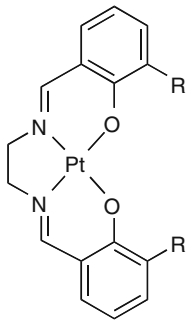

11 R = –H

13 R = –OCH3

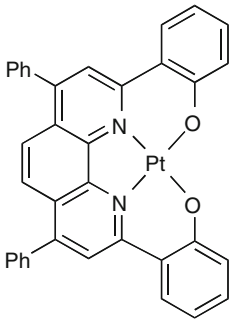

12

Wong and co-workers have recently described the result of intriguing intermolecular packing effects in a dimethoxy-substituted salen complex **13** [38, 39]. For example, different solvates have been crystallised, **13**.H_2O and **13**.DMF, which are orange and red respectively. The very different packing arrangements in the two crystals are shown in Fig. 9a, b. Meanwhile, the self-assembly of **13** with $K_2Pt(CN)_4$ or $K_2Pd(CN)_4$ leads to compounds $[K_2(\mathbf{13})_2M(CN)_4]$ (M = Pd or Pt, isostructural; Fig. 9c). K–O coordination in the crystals of these compounds brings the **13** units

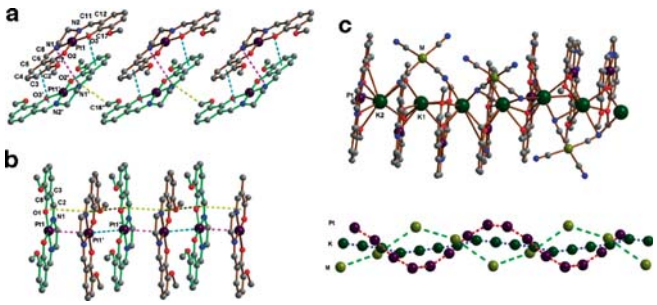

Fig. 9 Packing of the molecules in the crystals of (**a**) **13**.H_2O and (**b**) **13**.DMF, from X-ray diffraction analysis. Hydrogen atoms are omitted for clarity. (**c**) The packing and one-dimensional helical chains observed in the structures of $[K_2(\mathbf{13})_2 M(CN)_4]$ (M = Pd or Pt). Reprinted from [38] with permission from Elsevier

closer together than in the two solvates, probably accounting for the greater red component in the solid-state emission spectrum of the former compounds [38].

5 Pt(N^N⁻)-Based Complexes: 'Pseudo-Cyclometallates'

Whereas pyridines and quinolines necessarily bind to metal ions as neutral two-electron 'L' donors, heterocycles such as pyrazole, indazole, imidazole and triazole can do so either via a neutral nitrogen atom or through deprotonation of a 'pyrrolic' nitrogen, as does pyrrole itself. Bidentate ligands that incorporate each type of ring, for example 3-(2-pyridyl)pyrazole, can thus frequently bind either as N^N or N^N⁻ ligands (Fig. 10). In the latter case, the coordination offered to the metal is essentially analogous to that of a cyclometallating ligand such as 2-phenylpyridine (ppy), and the resulting complexes could be construed as pseudo-cyclometallates, in which the N⁻ atom resembles a metallated carbon. Since such ligands should exert a strong ligand field, a beneficial effect on luminescence efficiencies might be anticipated.

Chi and co-workers have explored the chemistry of platinum(II) with a series of 3-(2-pyridyl)pyrazole, 3-(pyrazyl)pyrazole and 3-(2-pyridyl)triazole ligands, and have noted that their luminescence quantum yields in solution vary widely according to the identity of substituents on the rings [40]. For example, the *tert*-butyl-substituted complexes **14** and **15** are amongst the most intensely luminescent platinum(II) complexes known ($\Phi = 0.82$ and 0.86; $\tau = 2.4$ and 2.1 μs respectively). In contrast, the analogues **16a** and **16b**, incorporating fluorinated substituents, and the triazole systems **17a** and **17b** display only very weak and short-lived emission under the same conditions ($\Phi < 10^{-3}$; $\tau < 10$ ns), possibly due to severe self-quenching. Nevertheless, bright emission is observed from thin solid films of these compounds, probably due to aggregation to give a Pt_2 $d\sigma^* \rightarrow \pi^*$(N^N) excited state. This assignment is supported by the short Pt···Pt contacts (3.442 Å) in the

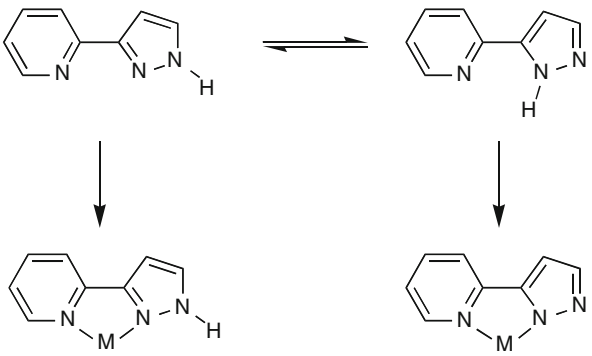

Fig. 10 The tautomeric forms of 3-(2-pyridyl)-pyrazole can allow it to coordinate to a metal M as either a neutral N^N-binding ligand, or as an anionic N^N⁻ ligand, analogous to a cyclometallating N^C ligand

crystal structure of **16b**, compared to a displaced arrangement of the molecules in the structure of **15**, where Pt···Pt distances are too long for significant interaction of d_{z2} orbitals. Both types of complexes have been successfully incorporated into electroluminescent devices by doping into a CBP host; e.g. an external quantum efficiency of 6% was observed in such a device employing **16a**.

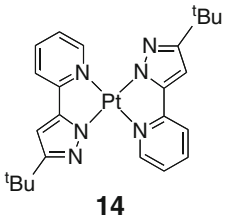

14

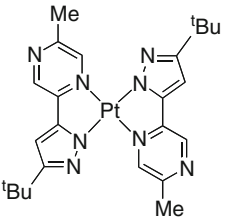

15

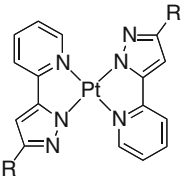

16 **a** R = CF_3
b R = C_3F_7

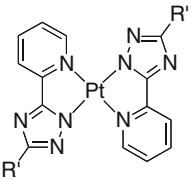

17 **a** R' = ^{t}Bu
b R' = C_3F_7

The change from N^N to N^N$^-$ and the beneficial effect this can have on luminescence efficiency is dramatically illustrated by the platinum(II) complexes of a pair of isoquinolyl–indazole ligands also investigated by Chi [41]. The complexes in which these ligands are bound as neutral N^N ligands, **18** and **19**, are non-emissive in solution, just like Pt(bpy)Cl_2. However, upon reaction with anionic ligands such as picolinate or a pyridylpyrazolate, deprotonation of the indazolic N–H occurs to give N^N$^-$-bound complexes, e.g. **20** and **21**. These complexes are luminescent in solution at room temperature, a change that can be attributed to the increase in ligand field strength that accompanies deprotonation. The 1-linked isomers are consistently better emitters than the 3-linked isomers (e.g. Φ_{lum} = 0.64 and 0.035, τ = 8.2 and 0.85 μs for **20** and **21** respectively, in CH_2Cl_2 at room temperature), which seems to be related primarily to faster non-radiative decay in the latter.

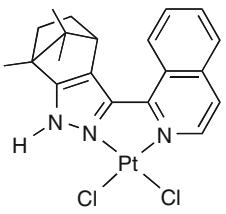

18

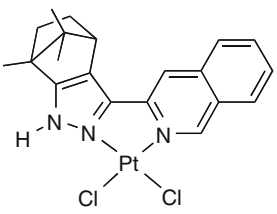

19

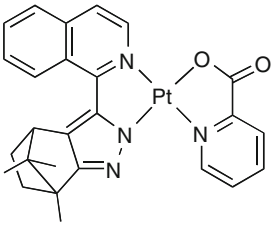

20

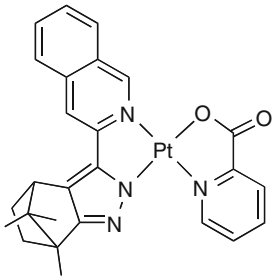

21

Pyrroles can function in a similar way to the deprotonated pyrazoles of the above systems, when incorporated into chelating ligands reminiscent of salen, as demonstrated by Che and co-workers [42]. They prepared the complexes **22**–**24** which display the emission spectra shown in Fig. 11. Solution quantum yields of **22** and **23** are of the order of 0.10 (in MeCN at 298 K), while the shift to lower energy in the phenylene-based system **24** – associated with the more extended π-conjugated system – is accompanied by reduction in Φ_{lum} to 0.001. OLEDs incorporating **22** and **23** doped into a CBP emissive layer have been fabricated. In the case of **22**, the spectral output is dependent on dopant concentration, λ_{max} increasing from 580 to 620 nm on going from 0.8 to 6.0 wt%. This change is attributed to excimer or oligomer formation at the higher loadings. Notably, the colour coordinates (0.62, 0.38) of the 6% system are close to those for pure red light (0.65, 0.35). No such concentration dependence is observed for **23**, probably because the methyl groups inhibit the close approach of the molecules that is necessary for the oligomer or excimer to form.

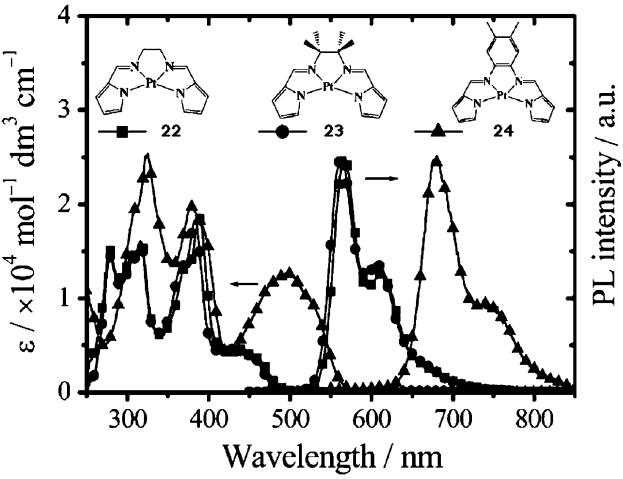

Fig. 11 Structural formulae of **22**–**24** and their absorption and photoluminescence spectra in MeCN at 298 K. Reprinted from [42] with permission from RSC

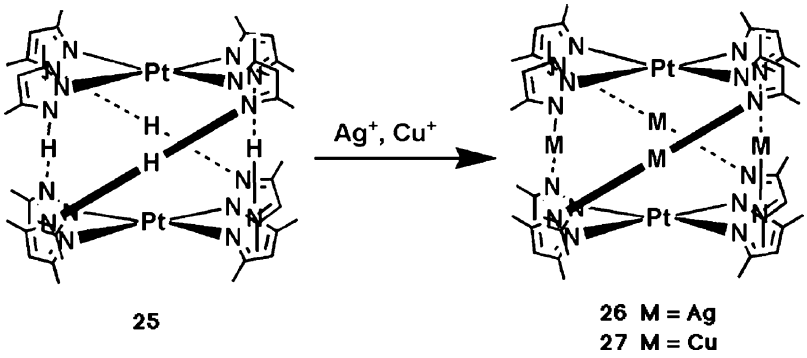

Fig. 12 The synthesis of **26** and **27** by treatment of **25** with Ag^+ or Cu^+ respectively

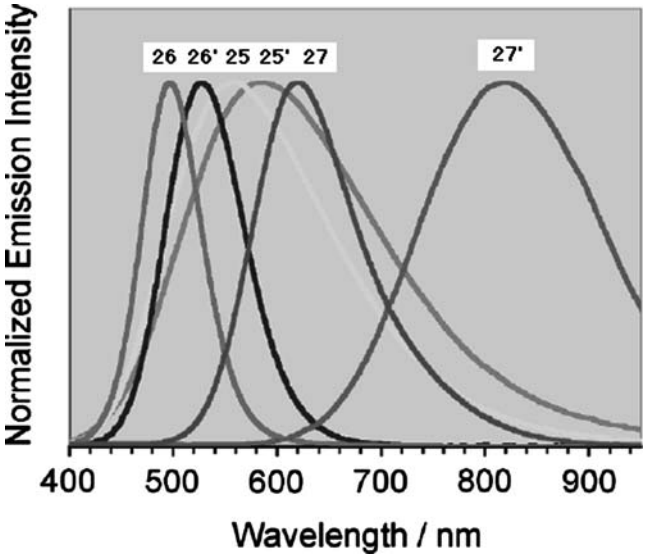

Fig. 13 Normalised emission spectra of **25**, **26** and **27** in the solid state (no prime) and in CH_2Cl_2 at 295 K (prime), $\lambda_{ex} = 266$ nm. Reprinted from [43] with permission from ACS

Platinum-containing heteropolynuclear complexes based on deprotonated pyrazoles have recently been reported by Umakoshi et al. [43]. These intriguing compounds have formulae $[Pt_2M_4(\mu\text{-}Me_2pz)_8]$ (M = Ag or Cu; **26** and **27** respectively), and are prepared from the corresponding protonated systems (M = H, **25**) (Fig. 12) {Me_2pz = 3,5-dimethylpyrazolate). The compounds **25**, **26** and **27** display yellow, blue and orange luminescence (Φ_{lum} = 0.06, 0.85 and 0.28) respectively, in the solid state at 295 K. They also emit in solution, although substantially more weakly, probably because of significant structural changes accompanying the formation of the excited state, as suggested by the large red-shifts in solution compared to the solid state (Fig. 13). DFT calculations highlight the importance of metal-metal bonding in the frontier orbitals and indicate that the microsecond emission of

26 and **27** can be assigned to states of $^3[Pt_2 \rightarrow Pt_2Ag_4]$ and $^3[Cu(d) \rightarrow Pt_2Cu_4]$ character respectively.

6 Pt(N^C)-Based Complexes (N^C = Bidentate Cyclometallating Ligand)

6.1 The 2-Arylpyridines and Analogues: Versatile Cyclometallating Ligands for Colour Tuning of Platinum(II) Complexes

The bis-cyclometallated complex Pt(N^C-thpy)$_2$ **28** (thpyH = 2-thien-2-ylpyridine), reported by von Zelewsky in the mid-1980s [44], was one of the first clear-cut examples of a simple platinum(II) complex that phosphoresces in fluid solution at room temperature ($\lambda_{max} = 578$ nm, $\tau = 2.2$ μs in a PrCN/MeCN mixture) [45]. Barigelletti et al. showed, by means of a study of the temperature dependence of emission, that the influence of cyclometallation is to displace the *d–d* state to about 3,700 cm^{-1} above the emissive state, ensuring that thermally-activated non-radiative decay is blocked off [46]. Although not thermally stable and hence not suitable for vacuum deposition methods of OLED fabrication, this complex and the trimethylsilyl derivative **29** has been incorporated into devices by spin-casting with TPD as a host material, and an EL efficiency of 11.5% has been achieved with **29** [47, 48].

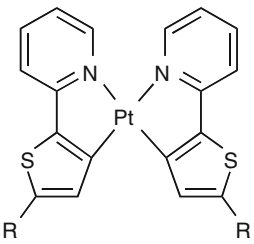

28 R = H

29 R = $SiMe_3$

The formation of such bis-cyclometallated complexes incorporating two such N^C ligands is not trivial, requiring the use of lithiated ligands, the formation of which is intolerant of many functional groups. In fact, complexes with just one such ligand and a second, coordinating (as opposed to metallated) bidentate ligand are excellent alternatives and are normally more readily prepared. For example, it is often possible to treat the N^C ligand with one equivalent of K_2PtCl_4 to generate a dichloro bridged dimer, (N^C)Pt(μ-Cl)$_2$Pt(N^C), which can then be cleaved with a variety of monodentate or bidentate ligands [49]. The dimers are usually formed readily in mixed solvent systems such as ethoxyethanol/water at 80°C. Reaction times are usually of the order of 24 h, although Ghedini and co-workers have recently reported that microwave irradiation can greatly speed up the reaction, provided that the temperature does not rise beyond about 65°C, which seems to induce degradation of the platinum salt [50].

Treatment with bidentate diamines, diimines or bis(pyrazolyl)borates gives $[Pt(N^C)(N^N)]^+$ monometallic complexes [16, 51]; bidentate anionic ligands L^X such as β-diketonates give neutral Pt(N^C)(O^O) [52]. Unidentate ligands can also be introduced to give, e.g. $[Pt(N^C)Cl_2]^-$, Pt(N^C)(CO)Cl, Pt(N^C)(CO)SR [16, 53, 54]. In fact, the choice of the other ligands is crucial to luminescence efficiency. For example, the ligand field strength in $[Pt(N^C)Cl_2]^-$ is inadequate to inhibit non-radiative decay via the *d–d* state, whereas diimine complexes such as $[Pt(N^C)(bpy)]^+$ are significantly emissive at room temperature. In the latter case, the bpy also influences the nature of the excited state, since the LUMO is largely localised on this ligand, leading to a d(Pt) → π*(N^N) excited state [16].

The β-diketonate class Pt(N^C)(O^O) (e.g. O^O = acac) have proved to be very popular, as the O^O ligand is easily introduced and normally does not influence the excited state energy significantly, so that the properties are essentially those associated with the N^C ligand. Thompson and co-workers carried out a landmark study of such systems with acac or its *tert*-butyl analogue dipivaloylmethane (dpm), in which 23 different N^C-coordinating ligands were investigated [52]. This study revealed that the d(Pt)/π(N^C) → π*(N^C) emission of these systems can be tuned over a wide range by relatively simple structural modification of the N^C ligand, in a way that is quite similar to that achieved over the past decade with N^C-based iridium(III) complexes. Briefly, electron-withdrawing substituents in the aryl ring and electron-donating substituents in the pyridine ring lower the HOMO and raise the LUMO respectively, leading to a shift to the blue. In contrast, extending the conjugation in the heterocycle through the use of quinolines, or using benzothiazole in place of phenyl as the cyclometallating ring, shifts the emission to the red. The extremes are represented by **30** and **31** which, at 77 K, have emission maxima of 440 and 600 nm respectively. Although many of the complexes also emit quite strongly at room temperature, this is not true for all; e.g. for **30**, $\Phi_{lum} < 10^{-3}$, possibly due to a small energy gap between the emissive and higher-lying *d-d* state.

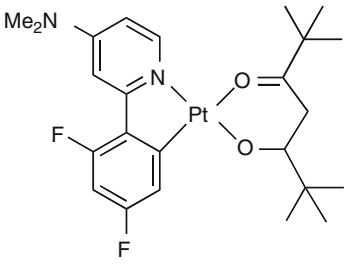

30

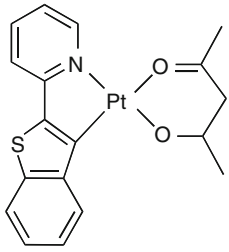

31

A series of related complexes incorporating styryl pendants **32a–d** (Fig. 14) have been investigated by Guerchais and co-workers, which display some rather intriguing properties arising from the possibility of *trans–cis* isomerisation of the

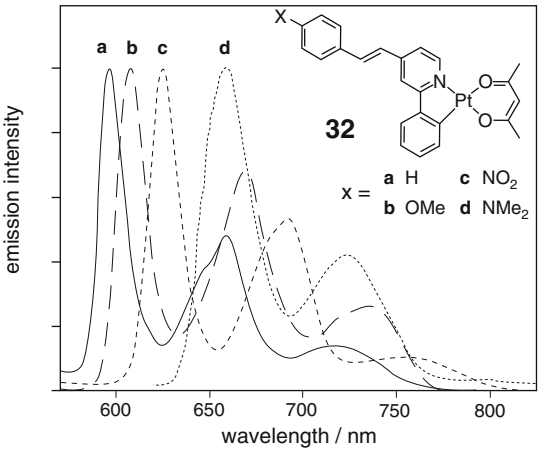

Fig. 14 The structures of the styryl-appended complexes **32a–d** and the long wavelength region of their emission spectra, where the *E* isomers emit, in an EPA glass at 77 K; $\lambda_{ex} = 400$ nm

C=C bond [55]. Emission is weak at room temperature, due to competitive C=C photoisomerisation, as confirmed by ^{1}H NMR spectroscopy. Little effect of the pendant on the emission energy is observed under these conditions, suggesting that the emissive state at room temperature is decoupled from the styryl group, perhaps indicative of a half-twisted –CH=CH– unit.

In contrast, in a rigid frozen glass at 77 K, two sets of bands with similar, well-defined vibrational progressions are observed, one in the region 460–560 nm, and the second set at substantially lower energy in the range 570–800 nm. These are assigned to the *cis* (*Z*) and *trans* (*E*) isomers respectively, evidence for which includes the change in their relative intensities according to the excitation wavelength. The former decrease in relative intensity as the excitation wavelength is increased from 350 to 430 nm, which correlates with the longer-wavelength absorption by the *E* isomer. The energy of the *E* bands is influenced by the substituent, as shown in Fig. 14, which reveals that the emission can be pushed right out to the far red by using an amine pendant [55].

In some complexes, the energy of the L^X ligand in Pt(N^C)(L^X) may be lower than that associated with the Pt(N^C) unit, in which case emission is likely to emanate from an L^X-based excited state. An example is provided by 8-quinolinol (the anion of 8-hydroxyquinoline, HQ) as a ligand, e.g. complex **33**. Here weak emission deep into the red is observed in solution at room temperature, which can

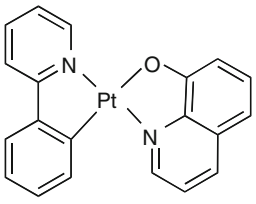

33

be further shifted to the NIR upon introducing substituents into the Q ligand [56, 57]. The emitting state has ILCT character, with a HOMO localised on the phenolate and LUMO on the pyridine ring of the same ligand, just as for the homoleptic complex Pt(quinolinol)$_2$ complexes investigated 30 years ago [58]. Despite the low quantum yield in solution (<0.01) and in powdered form (0.003), complex **33** has been doped into the emissive CBP layer of a multilayer OLED, giving a device displaying saturated red output (CIE coordinates 0.71, 0.28), albeit of efficiency that is too low to be practicable [59].

6.2 Excimers and Introduction to WOLEDs

As noted in Sect. 4.1, sterically unencumbered platinum(II) complexes may sometimes form excimers and/or aggregates, which emit at lower energy than the isolated monomeric molecules. In terms of applications to OLEDs, the combination of monomer and excimer emission from a single metal complex as dopant may offer an intriguing way forward in the development of white light-emitting devices (WOLEDs) [60]. Provisionally these have vast potential as efficient replacements of incandescent light bulbs and fluorescent strip lighting: around 22% of energy consumption in the U.S. is estimated to go on lighting [61]. White light is normally generated by using three separate emitters – red, green and blue [62]. If all three are combined within a single emitting layer, it can be difficult to control energy transfer from the higher energy blue to the green to red dye: energy tends to be 'short-circuited' to the lowest energy emitter. Segregation of the emitters into different layers can circumvent this problem, but this requires a more elaborate device architecture [63]. Thompson and Forrest put forward the novel approach of making use of a single phosphorescent dopant emitting simultaneously from monomer (blue–green) and excimer (green–red) states [60]. Clearly, Pt(II) complexes are potentially excellent candidates for this.

The trick is to achieve the right balance of excimer and monomer at the right sort of doping level, and this can be controlled to some extent through sterics. For example, photoluminescence spectra of a CBP host doped with increasing concentrations of Pt(N^C-F$_2$ppy)(acac) demonstrate that, at a low doping level of 1.5%, undesired residual emission from the host is observed in addition to that of the monomeric Pt complexes [64]. As the doping level is increased, the excimer emission rapidly appears and dominates at levels >8%, which is too low to achieve colour-balanced emission in a practicable device. If the complex is made more bulky to inhibit partially excimer formation, the onset of excimer emission can be limited to higher concentrations. The dpm (dpmH = dipivaloylmethane) derivative is *too* bulky: almost exclusively monomeric emission is observed even at 20% doping level. The mhpt complex, on the other hand, offers just the right level of steric bulk for balanced emission at 10% doping, and this behaviour has been successfully extrapolated to an electroluminescent device (Fig. 15) (mhptH = 6-methyl-2,4-heptanedione). The CIE coordinates of this device (0.36, 0.44) are

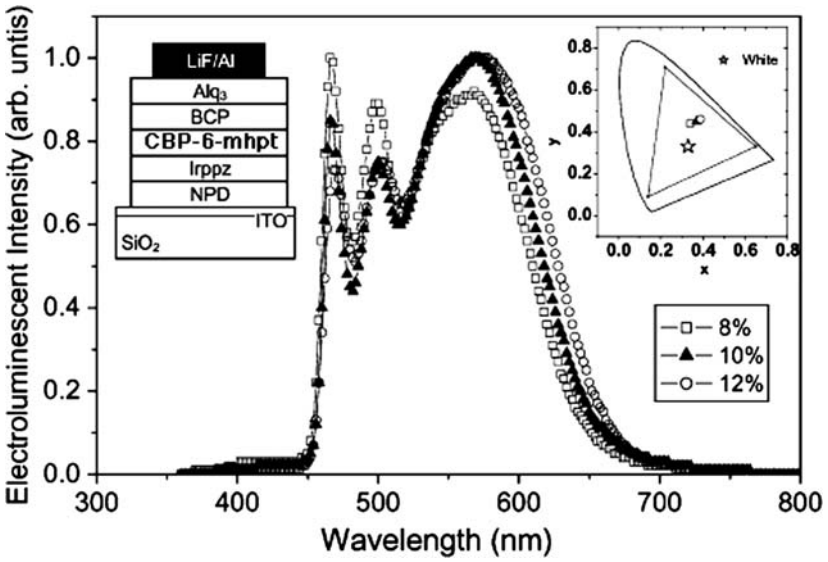

Fig. 15 Electroluminescence spectra and CIE coordinates for Pt(F2ppy)(mhpt) incorporated into the emissive layer of the multilayer device represented schematically in the inset, at the % dopings by mass indicated. Reproduced from [64] with permission from RSC

close to those for white light (0.33, 0.33), with a maximal efficiency of 3.3 ± 3 photons/electron at 0.5 cd m^{-2} [64].

6.3 Multifunctional Complexes

In most devices, the emissive layer is sandwiched between hole- and electron-transporting layers, in order to achieve balanced injection and transport of holes and electrons to optimise charge recombination within the EL layer. Wong et al. have been investigating multifunctional Pt emitters in which oxadiazole and triarylamine units are covalently linked to a Pt(ppy)(acac) emissive centre, to act as electron- and hole-transporting units respectively, e.g. **34** [65]. These sublimable compounds have been used to prepare neat-emissive-layer devices by vacuum evaporation between an ITO/CuPC anode and Ca/Al cathode. Molecules such as **34** display fluorescence from the arylamine as well as Pt-based phosphorescence, both in solution and when doped in the CBP emissive host. The ratio of fluorescence to phosphorescence can be controlled according to either the applied voltage (the blue colour intensity increases relative to the orange as the voltage increases), or the concentration of the dopant (intermolecular quenching of triplet excitons at high loadings leads to an increase in the proportion of blue component). Under appropriate conditions, the combination of the two contributions can be tuned to give WOLEDs, offering an alternative to the monomer-excimer approach [66].

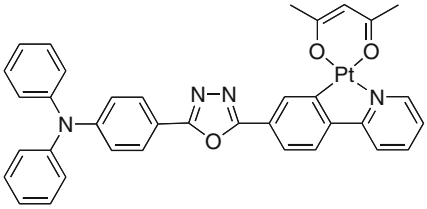

34

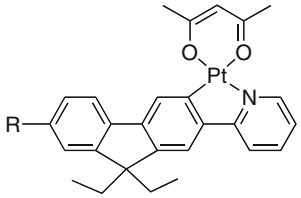

35

a R = Ph_2N–

b R = (p–Me–C_6H_4)$_2$N– **c** R = H–

Structurally analogous molecules incorporating fluorene instead of the oxadiazole have been prepared by the same group **35a–c** [67]. Again, the introduction of diarylamino substituents onto the fluorene leads to ILCT singlet fluorescence in addition to the Pt-based phosphorescence (Fig. 16). Notably, the 77 K phosphorescence lifetimes of the substituted systems are significantly longer than the unsubstituted analogue, in line with a smaller contribution of metal character in the excited state of these more extended systems, even though the triplet excited state energies are essentially unaffected.

Finally, we note that Marder and co-workers have recently reported on the covalent incorporation of Pt(N^C)(O^O) complexes into a polymer by ring opening metathesis copolymerisation of norbornene-appended complexes, e.g. **36**, with a norbornene-appended carbazole **37** [68]. Such an approach could provide

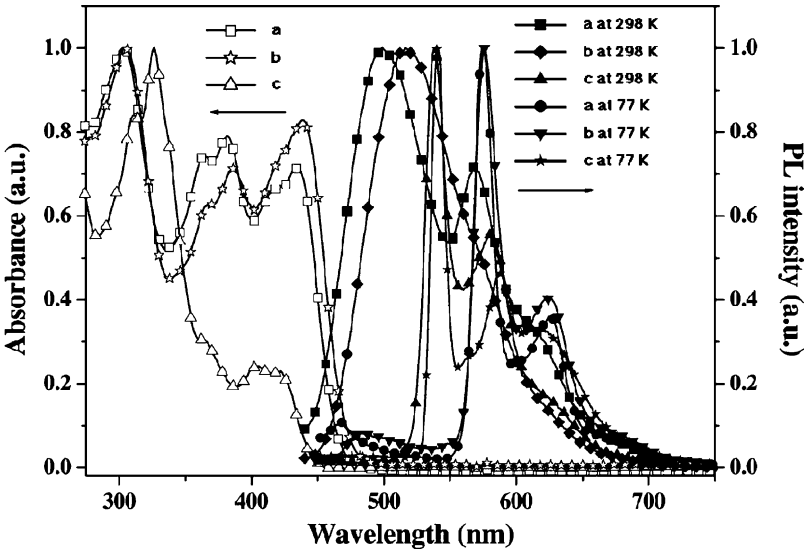

Fig. 16 Absorption and photoluminescence spectra of **35a–c** in CH_2Cl_2. Reprinted from [67] with permission from ACS

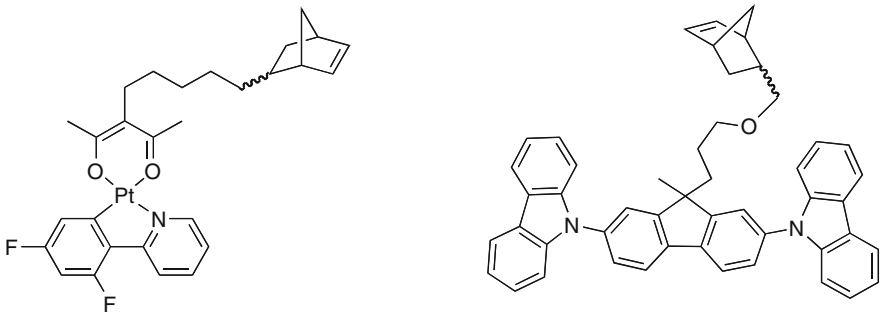

36 **37**

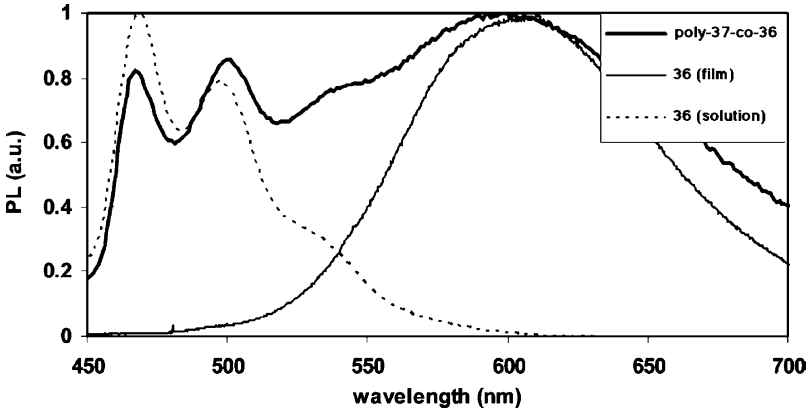

Fig. 17 Photoluminescence spectrum of a film of copolymer **37**-**co**-**36**, and corresponding spectra of monomer **36** as a thin film and in dilute solution in THF. Reprinted from [68] with permission from ACS

a solution to some of the problems associated with phase separation in blends of small-molecule phosphors and polymers. The photoluminescence spectra of the films formed in this way display both monomeric and excimer/aggregate emission (Fig. 17), as also proves to be the case in the electroluminescent devices.

7 Complexes with Terdentate Ligands

The *d*–*d* excited states of d^8 complexes comprising bidentate ligands are unstable with respect to distortion away from the D_{4h} symmetry of the ground state towards a D_{2d} symmetry, in which the plane of the bidentate ligand is twisted relative to that containing the other two ligands [69]. As highlighted in Fig. 3, excited state

distortion is associated with increased non-radiative decay, with an adverse effect on luminescence quantum yields. Terdentate ligands analogous to bpy and ppy, able to bind via three rings instead of two in a planar conformation, should in principle inhibit such distortion owing to a more rigid binding [70]. However, the bite angle associated with many such ligands, e.g. terpyridine (tpy), is not ideal for larger metal ions, leading to a weaker ligand field compared to that which might be anticipated. Thus, $[Pt(tpy)Cl]^+$, for example, is not emissive at room temperature, because the *d–d* state is low in energy [71]. Again, however, the introduction of stronger-field co-ligands in place of Cl can circumvent this problem, and a wide range of emissive complexes based on the $[Pt(tpy)(–C{\equiv}C–R)]^+$ structure have been investigated. The reader is directed to recent reviews on such systems by Castellano et al. and by Wong and Yam [15, 72]. In this contribution, our focus is on charge-neutral systems, which are more relevant to the topic of OLEDs. A variety of charge-neutral Pt(II) complexes have been obtained by employing cyclometallating terdentate ligands in combination with an anionic fourth ligand, selected examples of which are discussed in the sections that follow.

7.1 Platinum(II) Complexes with N^N^C-Binding Ligands

Che and co-workers have pioneered much of the work on cyclometallated Pt(II) complexes with the N^N^C-coordinating ligand, 6-phenylbipyridine (phbpyH) and derivatives [73]. Of particular interest is their comprehensive study of around 30 such complexes incorporating σ-alkynyl ligands in the fourth coordination site of the metal ion, [Pt(N^N^C)(–C≡C–R)] [74]. The majority of the complexes are emissive in solution at room temperature, giving featureless spectra ranging from green to red. The emission in most of the systems is attributed to a ^{3}MLCT ($d_{Pt} \rightarrow \pi^*_{NNC}$) state, an assignment that is supported by the influence of structural modification of both the N^N^C ligand and the acetylide on the emission properties. For example, for a series of *p*-substituted aryl acetylides **38**, the emission maximum shifts to higher energy as the substituent X becomes more electron-withdrawing, and the metal-based HOMO is lowered in energy (Fig. 18). A good negative linear correlation of log Σk_{nr} with the emission energy illustrates that the energy gap law is obeyed within this series (Fig. 18, inset). Meanwhile, introduction of electron-donating *tert*-butyl groups into the 4-positions of the pyridyl rings of the N^N^C ligand shifts the emission energy to the blue (**39**, R = *t*-Bu vs. R = H), whilst an ester at this position (**39**, R = $–CO_2Et$) has the opposite effect, reflecting the contrasting influence of these substituents in raising and lowering the LUMO energy respectively. Substituents in the cyclometallating phenyl ring were found to have rather little influence, but changing from phenyl to thienyl or furanyl rings (**40**, X = S or O), led to a substantial red shift in emission, which can be attributed to the more electron-rich nature of these heterocycles. The complexes are thermally stable and a number of them have been incorporated successfully into OLEDs.

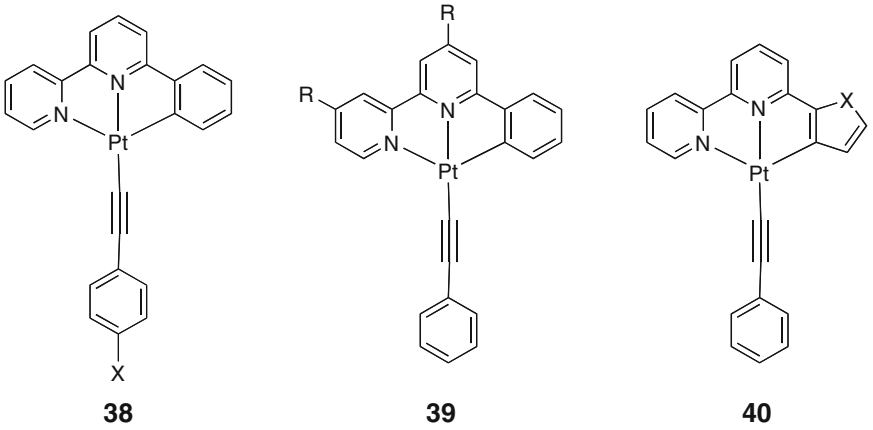

38 **39** **40**

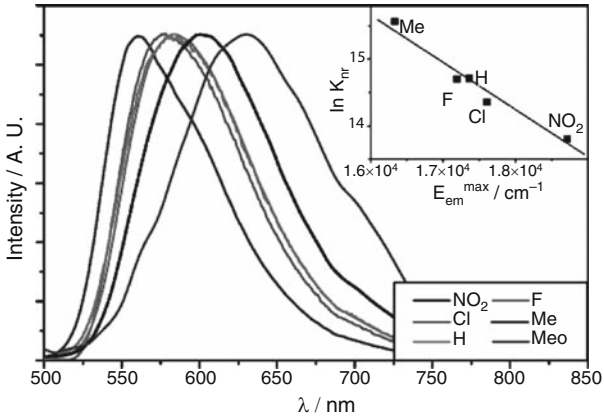

Fig. 18 Normalised emission spectra of complexes of type **38,** carrying the different X groups indicated, in dichloromethane at 298 K. In order of increasing λ_{max}: X = NO_2 < Cl < H = F < Me < MeO. *Inset*: plot of ln Σk_{nr} vs the energy corresponding to the respective emission maxima. Reprinted from [74] with permission from ACS

Interestingly, in some cases, a switch to ^{3}LC excited states localised on the acetylide or on the aryl group of the acetylide can be achieved. For example, Fig. 19 shows the influence of polyacetylide ligands: on going from the $n = 3$ to $n = 4$ system **41**, a dramatic switch to a highly structured acetylide-localised state is observed. Similarly, when a 2-pyrenylacetylide ligand is used, the lowest-lying excited state is the ^{3}LC state associated with the pyrenyl moiety, which emits deep into the red (λ_{max} 664 nm).

A somewhat related complex incorporating a pyrenyl unit has been reported recently by Li and Yang, but in this case the pyrenyl unit is substituted onto the central 4-position of the N^N^C ligand, **42** [75]. In this compound, dual emission is

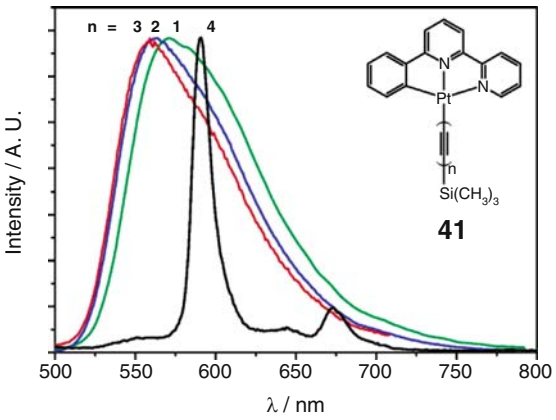

Fig. 19 The influence of extending the polyacetylide ligand in the generic structure shown, revealing the switch from ^{3}MLCT to ^{3}LC emission that occurs at $n = 4$. Reprinted from [74] with permission from ACS

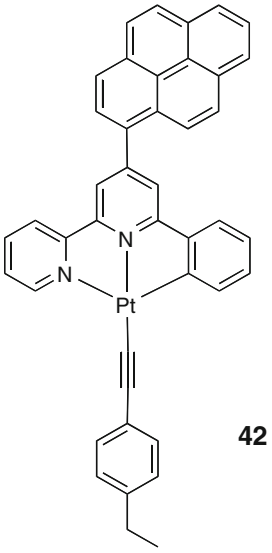

42

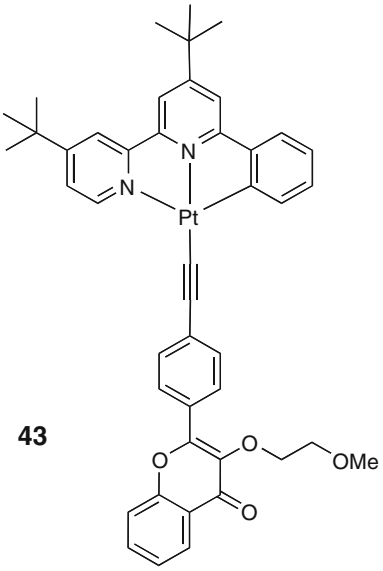

43

observed from both ^{3}MLCT ($d_{Pt} \rightarrow \pi^*_{NNC}$) and pyrenyl-based $^3\pi$–π^* states, both at 77 K and – unusually – at room temperature. The grow-in and decay kinetics of the two bands, in conjunction with transient absorption spectroscopy, reveal that the pyrenyl $^3\pi$–π^* state is largely populated directly by intersystem crossing from the ^{1}MLCT state, as is the ^{3}MLCT state, whereas the triplet–triplet internal conversion of the ^{3}MLCT state to the pyrenyl $^3\pi$–π^* state is of negligible importance.

Fillaut et al. have also observed emission from a 'remote' π–π^* state in the complex **43**, where long-lived emission ($\tau \sim 18$ μs) centred around 570 nm is associated with the flavonol unit, whose triplet emission is promoted by coupling to the platinum centre [76]. Interestingly, when the flavonol binds divalent metal

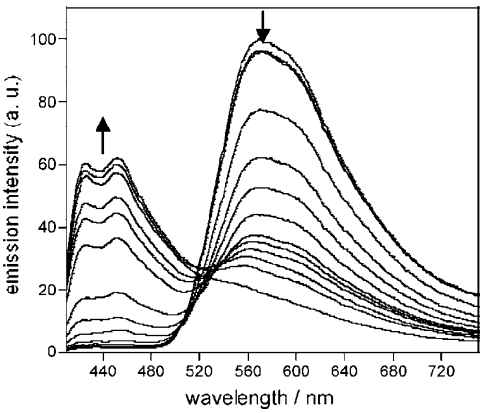

Fig. 20 Luminescence spectral changes of **43** (10^{-5} M) in MeCN upon addition of $Pb(ClO_4)_2$ (λ_{ex} = 393 nm) [76]

ions, particularly Pb^{2+}, the relative energies of the excited states change such that the two parts of the molecule become decoupled, and emission then switches to being flavonol-based fluorescence (Fig. 20).

McMillin and co-workers have recently reported on the platinum(II) complex of an N^N^C-coordinating ligand that incorporates a phenazine in the backbone, **44**, together with its cationic N^N^N analogue **45** [77]. They investigated the influence of Lewis acids and bases on the emission. The emission of both complexes is quenched by Lewis bases, as frequently observed for simple Pt(II) complexes, and rationalised on the grounds of sterically accessible attack at the coordinatively unsaturated Pt centre. However, the emission of **44**, but not of **45**, is also quenched by acid. This difference is attributed to the greater degree of charge-transfer character in the cyclometallated system, which is also manifest in its substantially shorter excited state lifetime (τ = 270 ns in chloronaphthalene compared to 5 μs for **45** in dichloromethane).

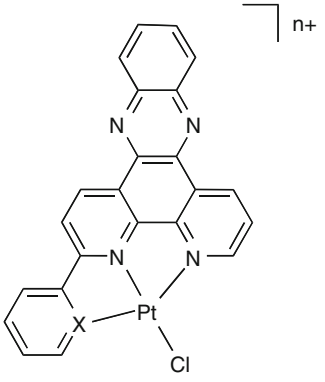

44 X = C, n = 0

45 X = N, n = 1

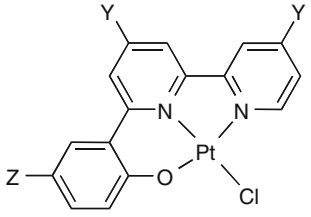

46

7.2 Platinum(II) Complexes with N^N^O-Binding Ligands

As noted in Sect. 4.3, the combination of diamine or diimine and phenolic donors in salen and related ligands can lead to emissive complexes. In the same way, the aryl ring of N^N^C-based complexes can be replaced by an *ortho*-phenolate. Thus, a range of luminescent N^N^O-coordinated complexes based on the 6-(2-hydroxyphenyl)-2,2'-bipyridine, have been synthesised by Che and co-workers, **46** (where Y = H, Me or t-Bu; Z = H or F) [78]. In fact, the parent ligand was initially isolated as a side product of the synthesis of the bpy-based analogue of the tetradentate ligand in complex **12**, but the terdentate ligand also proved successful at forming thermally stable, emissive complexes. Broad orange–red emission at room temperature again originates from a mixed $d_{Pt}/p_O \rightarrow \pi^*_{N^N}$ excited state. When incorporated into OLEDs, good performance yellow devices were obtained. Although dopant concentration did not affect the device colour, the presence of fluorine and *tert*-butyl at positions Z and Y respectively was found to give the highest efficiency.

7.3 Platinum(II) Complexes of N^C^N-Binding Ligands

Our group has been investigating complexes of 1,3-di(2-pyridyl)benzene (dpybH) and derivatives. The parent system **47** (Y = Z = H) is the isomer of the N^N^C-coordinated complex (Sect. 7.1). However, the positioning of the cyclometallating aryl ring in the central rather than lateral position within the terdentate system leads to improved luminescence efficiency (e.g. $\phi = 0.60$ for the parent compound), probably due to the increased ligand field strength associated with the shorter Pt–C bond [79]. The highly structured emission that is scarcely shifted in position nor elongated in lifetime upon cooling to 77 K is suggestive of a primarily ligand-centred π–π* state, in which the contribution of the metal is nevertheless sufficient to promote the triplet emission. These conclusions are supported by DFT calculations [10], which reveal a HOMO that spans the cyclometallating ring, the metal and the chloride co-ligand, and a LUMO that is localised on the pyridine rings.

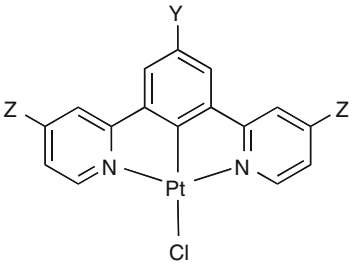

47

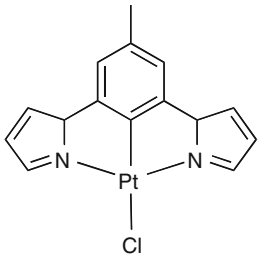

48

This localisation of frontier orbitals also accounts for the influence of substituents on emission energy. For example, the introduction of aryl substituents into the central 4-position (Y) of the central ring leads to a lowering in the excited state energy, both the singlet state (E_{abs}) and triplet (E_{em}). A good linear correlation of both E_{abs} and E_{em} is observed with the oxidation potential, which can be understood in terms of the influence of increasingly electron-rich pendants in raising the HOMO level, whilst the LUMO is largely unaffected (Fig. 21) [80]. In the case of the most electron-rich amine substituents (e.g. R = $-C_6H_4-NMe_2$), however, the emissive excited state is stabilised more than anticipated on the basis of the oxidation potential, an observation that has been attributed to a switch to an ICT-type state, involving a high degree of charge transfer, and manifest through the pronounced solvatochromism observed in emission [80, 81]. Reversible switching between the localised and charge-transfer states can be induced by protonation, and the effect can be extrapolated to azacrown pendants that bind divalent metal ions [81].

Whilst the above strategy of introducing electron-rich pendants successfully lowers the excited state energies, scope for shifting to the blue through modification at this position is more limited; an electron-withdrawing ester group leads to a shift of 10 nm. However, further blue shifts have been accomplished by introducing electron-donating substituents into the pyridyl rings, particularly the 4-position, which raise the LUMO energy [82]. Another way of achieving the same effect is to change from pyridine to pyrazole rings, which are poorer π-acceptors. Thus, the emission of complex **48** is blue-shifted by 1,700 cm^{-1} compared to that of **47**,

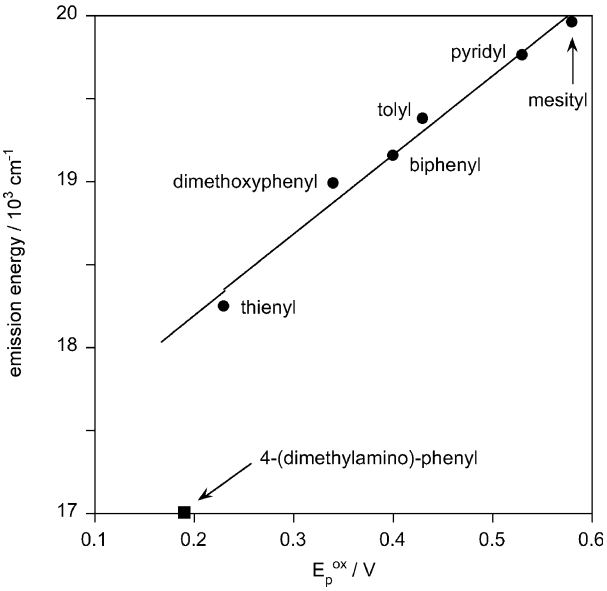

Fig. 21 Correlation of the emission energy E_{em} of complexes of type **47** (Z = H), carrying the aryl substituents indicated at position Y, with the oxidation peak potential measured by cyclic voltammetry in CH_2Cl_2 [80]

though unfortunately accompanied by a substantial decrease in the emission quantum yield [83].

As for the ppy-based systems discussed in Sect. 6.2, the majority of the N^C^N-coordinated complexes display very efficient excimer formation, and the excimers themselves are remarkably highly emissive ($\Phi \sim 0.3$). By varying the dopant concentration within the host emissive layer, the ratio of monomeric (blue) to excimeric (red) emission is varied, and the observed light that the device produces is the net combination. At a doping level of 15% in a CBP host, a device has been obtained that emits with CIE coordinates of 0.337, 0.384, close to white light, and with a quantum efficiency of 18.1%, making it one of the most efficient WOLEDs reported hitherto [84].

In fact, the camel-shaped spectrum leads to a trough of low emission intensity between the monomer and excimer regions, making the coverage across the visible less uniform than might be desirable. Kalinowski et al. have found that this problem can be overcome by 'filling in' this region with emission from an exciplex [85, 86]. The concept is illustrated in Fig. 22. In the emitting region, a starburst amine hole-transporting bathophenanthroline (m-MTDATA) acts as an electron donor (D) to the Pt complex **47** (Y = $-CO_2Me$) as an electron acceptor (A), mixed in a 1:1 ratio. Monomer phosphor triplets, ^{3}A*, their corresponding excimers ^{3}(AA)* formed upon encounter with ground state A, and excited hetero-dimers, i.e. exciplexes, ^{3}(DA)*, are generated throughout the emissive layer. A colour rendering index of 90 with an external quantum efficiency of 6.5% photons/electron has been attained in this way [85]. The phenomenon of electro-photoluminescence in organics has also been demonstrated for the first time recently using **47** (R = $-CO_2Me$) [87].

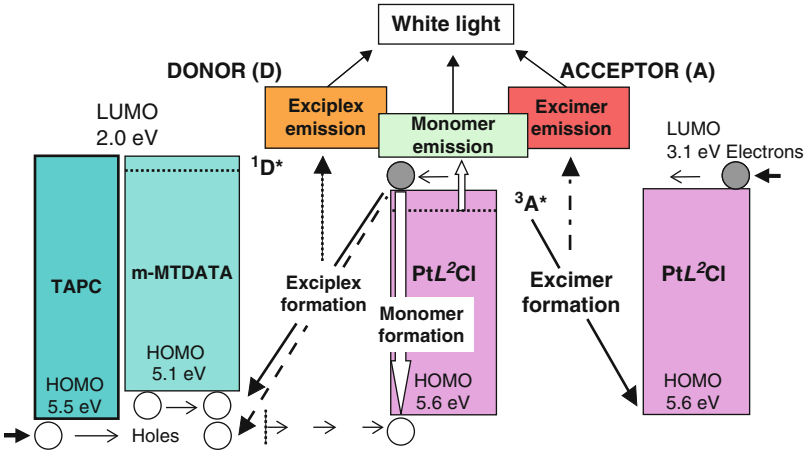

Fig. 22 Generation mechanisms of white light in an OLED based on a hole transporting material (m-MTDATA) acting as an electron donor (D) to an electron acceptor (A) molecule of an organic phosphor (**47** R = CO_2Me) mixed in an emissive layer, D:A. The monomer phosphor triplets (^{3}A*), their combination with ground state phosphor acceptor molecules [triplet excimers, ^{3}(AA)*], and excited hetero-dimer [^{3}(DA)*] are generated throughout the emissive layer leading to white light with colour rendering indices (CRI) up to 90 [85]

These highly emissive complexes have also been applied in sensory applications. Although quenched by O_2, they are not quenched as efficiently as longer-lived systems such as platinum porphyrins. Thus, by combining a thin layer of green-emitting Pt(N^C^N) with a second layer of red-emitting platinum porphyrin in ethyl cellulose, a traffic light response system to O_2 has been developed, in which the system emits red light in the absence of O_2, turning orange and then green as pO_2 increases, and the porphyrin becomes quenched more than the N^C^N complex [88]. Very recently, the simplest complexes of this type have also been shown to be successfully applicable to time-resolved imaging in live cells on the microsecond timescale (Fig. 23) [89]. The parent complex is highly cell permeable, entering essentially under diffusion control, and localises to the nucleoli (Fig. 24). It is also amenable to two-photon excitation in the near-IR.

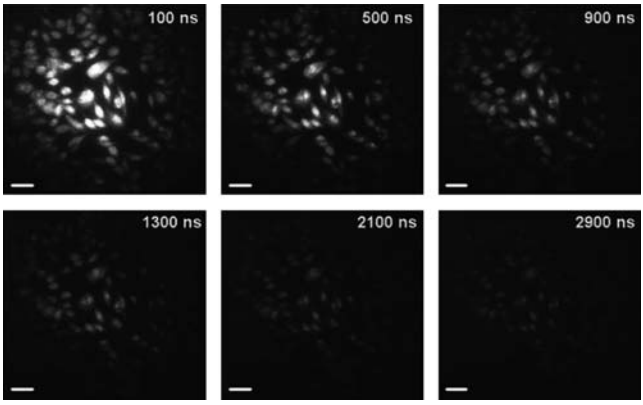

Fig. 23 Time-resolved gated emission images of CHO cells incubated with **47** (Y = Z = H). The images were recorded after 355 nm laser excitation at the time delays shown between 100 and 2,900 ns after the laser flash. The time gate used was 100 ns, exposure time 0.02 s, five accumulations per time delay. *Scale bar*: 50 μm [89]

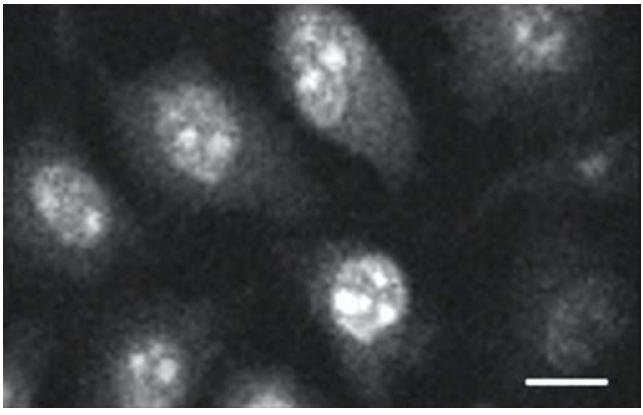

Fig. 24 A two-photon excitation high-resolution emission image of live CHO cells incubated with **47** (Y = Z = H), obtained under 758 nm 180 fs excitation. *Scale bar* = 10 μm [89]

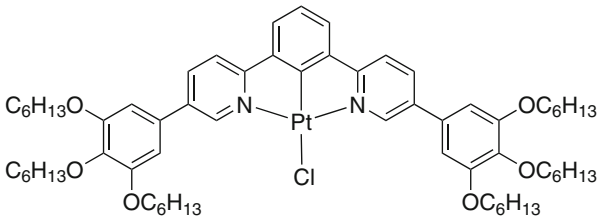

49

Meanwhile, Bruce and co-workers have appended complexes of this type with long alkyl chains, adding interesting liquid crystalline (LC) properties to the luminescence. For example, the properties of an LC state of **49**, obtained by slowly cooling from the isotropic melt to 170°C then rapidly cooling to room temperature, were compared with a non-crystalline phase formed from rapid cooling of the isotropic melt. Structural analysis revealed that the LC phase was composed of a columnar phase of anti-parallel complexes which are independent of one another. The non-crystalline phase, in contrast, consists of a high degree of isotropic grain boundaries, and molecules are therefore in close contact. As a result, emission from the LC state is purely monomeric, and emission from the non-crystalline phase is purely excimeric (Fig. 25). In some cases, reversible thermally-induced switching of excimer to monomer in spin-coated thin films has also been observed [90].

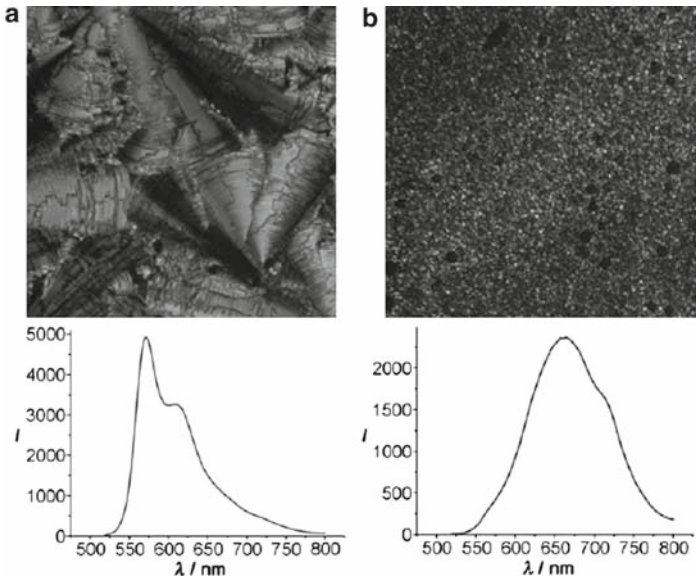

Fig. 25 Photomicrographs taken between cross polarisers (*top*) and emission spectra (*bottom*) of **49** (**a**) fast cooled from the LC phase after the texture is developed, and (**b**) fast cooled from the isotropic phase. Reprinted from [90] with permission from Wiley

References

1. Lakowicz JR (2006) Principles of fluorescence spectroscopy, 3rd edn, chap 1. Springer, Berlin Heidelberg New York
2. Montalti M, Credi A, Prodi L, Gandolfi MT (2006) Handbook of photochemistry, 3rd edn. Taylor & Francis, Boca Raton
3. Hung LS, Chen CH (2002) Mater Sci Eng R 39:143–222
4. Wilson JS, Köhler A, Friend RH, Al-Suti MK, Al-Mandhary MRA, Khan MS, Raithby PR (2000) J Chem Phys 113:7627–7634
5. Baldo MA, O'Brien DF, You Y, Shoustikov A, Sibley S, Thompson ME, Forrest SR (1998) Nature 395:151–154
6. Thompson ME, Burrows PE, Forrest SR (1999) Curr Opin Solid State Mater Sci 4:369–372
7. Danilov EO, Pomestchenko IE, Kinayyigit S, Gentili PL, Hissler M, Ziessel R, Castellano FN (2005) J Phys Chem A 109:2465–2471
8. Michalec JF, Bejune SA, McMillin DR (2000) Inorg Chem 39:2708–2709
9. Hu J, Lin R, Yip JHK, Wong K-Y, Ma D-L, Vittal JJ (2007) Organometallics 26:6533–6543
10. Sotoyama W, Satoh T, Sato H, Matsuura A, Sawatari N (2005) J Phys Chem A 109:9760–9766
11. Williams JAG (2007) Top Curr Chem 281:205–268
12. Miskowski VM, Houlding VH (1989) Inorg Chem 28:1529–1533
13. Miskowski VM, Houlding VH, Che CM, Wang Y (1993) Inorg Chem 32:2518–2524
14. Eastwood D, Gouterman M (1970) J Mol Spectrosc 35:359
15. Castellano FN, Pomestchenko IE, Shikhova E, Hua F, Muro ML, Rajapakse N (2006) Coord Chem Rev 250:1819–1828
16. Kvam P-I, Puzyk MV, Balashev KP, Songstad J (1995) Acta Chem Scand 49:335–343
17. Williams JAG, Develay S, Rochester DL, Murphy L (2008) Coord Chem Rev 252:2596–2611
18. Che C-M, Wan K-T, He L-Y, Poon C-K, Yam VW-W (1989) J Chem Soc Chem Commun 943–944
19. Kunkely H, Vogler A (1990) J Am Chem Soc 112:5625–5627
20. Wan K-T, Che C-M, Cho K-C (1991) J Chem Soc Dalton Trans 1077–1080
21. DeSchryver FC, Collart P, Vandendriessche J, Goedeweeck R, Swinnen A, Van der Auweraer M (1987) Acc Chem Res 20:159–166
22. Kato M, Shishido Y, Ishida Y, Kishi S (2008) Chem Lett 37:16–17
23. Kunkely H, Vogler A (2006) Inorg Chem Commun 9:827–829
24. Keller HJ (ed) (1977) Chemistry and physics of one-dimensional metals. Plenum, New York
25. Miller JS (ed) (1982) Extended linear chain compounds. Plenum, New York
26. Exstrom CL, Sowa JR Jr, Daws CA, Janzen D, Mann KR (1995) Chem Mater 7:15–17
27. Buss CE, Mann KR (2002) J Am Chem Soc 124:1031–1039
28. Kato M (2007) Bull Chem Soc Jpn 80:287–294
29. Sun Y, Ye K, Zhang H, Zhang J, Zhao L, Li B, Yang G, Yang B, Wang Y, Lai S-W, Che C-M (2006) Angew Chem Int Ed 45:5610–5613
30. Zhou X, Zhang H-X, Pan Q-J, Li M-X, Wang Y, Che C-M (2007) Eur J Inorg Chem 2181–2188
31. Klein A, Kaim W (1995) Organometallics 14:1176–1186
32. Dungey KE, Thompson BD, Kane-Maguire NAP, Wright LL (2000) Inorg Chem 39:5192–5196
33. Nishida J, Maruyama A, Iwata T, Yamashita Y (2005) Chem Lett 34:592–593
34. De Crisci AG, Lough AJ, Multani K, Fekl U (2008) Organometallics 27:1765–1779
35. Ardasheva LP, Shagisultanova GA (1998) Russ J Inorg Chem 43:85–93
36. Che C-M, Chan S-C, Xiang H-F, Chan MCW, Liu Y, Wang Y (2004) Chem Commun 1484–1485
37. Lin Y-Y, Chan S-C, Chan MCW, Hou Y-J, Zhu N, Che C-M, Liu Y, Wang Y (2003) Chem Eur J 9:1263–1272
38. Lü X, Wong W-Y, Wong W-K (2008) Eur J Inorg Chem 523–528

39. Chai W-L, Jin W-J, Lü X-Q, Bi W-Y, Song J-R, Wong W-K, Bao F (2008) Inorg Chem Commun 11:699–702
40. Chang S-Y, Kavitha J, Li S-W, Hsu C-S, Chi Y, Yeh Y-S, Chou P-T, Lee G-H, Carty AJ, Tao Y-T, Chien C-H (2006) Inorg Chem 45:137–146
41. Chang S-Y, Kavitha J, Hung J-Y, Chi Y, Cheng Y-M, Li E-Y, Chou P-T, Lee G-H, Carty AJ (2007) Inorg Chem 46:7064–7074
42. Xiang H-F, Chan S-C, Wu KK-Y, Che C-M, Lai PT (2005) Chem Commun 1408–1409
43. Umakoshi K, Kojima T, Saito K, Akatsu S, Onishi M, Ishizaka S, Kitamura N, Nakao Y, Sakaki S, Ozawa Y (2008) Inorg Chem 47:5033–5035
44. Chassot L, Müller E, von Zelewsky A (1984) Inorg Chem 23:4249–4253
45. Maestri M, Sandrini D, Balzani V, Chassot L, Jolliet P, von Zelewsky A (1985) Chem Phys Lett 122:375–379
46. Barigelletti F, Sandrini D, Maestri M, Balzani V, von Zelewsky A, Chassot L, Jolliet P, Maeder U (1988) Inorg Chem 27:3644–3647
47. Cocchi M, Virgili D, Sabatini C, Fattori V, Di Marco P, Maestri M, Kalinowski J (2004) Synth Met 147:253–256
48. Cocchi M, Fattori V, Virgili D, Sabatini C, Di Marco P, Maestri M, Kalinowski J (2004) Appl Phys Lett 84:1052–1054
49. Black DSC, Deacon GB, Edwards GL (1994) Aust J Chem 47:217–227
50. Godbert N, Pugliese T, Aiello I, Bellusci A, Crispini A, Ghedini M (2007) Eur J Inorg Chem:5105–5111
51. Niedermair F, Waich K, Kappaun S, Mayr T, Trimmel G, Mereiter K, Slugovc C (2007) Inorg Chim Acta 360:2767–2777
52. Brooks J, Babayan Y, Lamansky S, Djurovich PI, Tsyba I, Bau R, Thompson ME (2002) Inorg Chem 41:3055–3066
53. Mdleleni MM, Bridgewater JS, Watts RJ, Ford PC (1995) Inorg Chem 34:2334–2442
54. Kovelenov YA, Blake AJ, George MW, Matousek P, Mel'nikov MY, Parker AW, Sun X-Z, Towrie M, Weinstein JA (2005) Dalton Trans:2092–2097
55. Yin B, Niemeyer F, Williams JAG, Jiang J, Boucekkine A, Toupet L, Le Bozec H, Guerchais V (2006) Inorg Chem 45:8584–8596
56. Shavaleev NM, Adams H, Best J, Edge R, Navaratnam S, Weinstein JA (2006) Inorg Chem 45:9410–9415
57. Niedermair F, Kwon O, Zojer K, Kappaun S, Trimmel G, Mereiter K, Slugovc C (2008) Dalton Trans 4006–4014
58. Ballardini R, Indelli MT, Varani G, Bignozzi CA, Scandola F (1978) Inorg Chim Acta 31: L423–L424
59. Yang C-J, Yi C, Xu M, Wang J-H, Liu Y-Z, Gao X-C, Fu J-W (2006) Appl Phys Lett 89:233506
60. D'Andrade BW, Brooks J, Adamovich V, Thompson ME, Forrest SR (2002) Adv Mater 14:1032–1036
61. U.S. Department of Energy (2003) Illuminating the challenges: solid state lighting program planning workshop report. US Government Printing Office, Washington DC
62. Kido J, Shionoya H, Nagai K (1995) Appl Phys Lett 67:2281–2283
63. Kido J, Kimura M, Nagai K (1995) Science 267:1332–1334
64. Adamovich V, Brooks J, Tamayo A, Alexander AM, Djurovich PI, D'Andrade BW, Adachi C, Forrest SR, Thompson ME (2002) New J Chem 26:1171–1178
65. Wong W-Y, He Z, So S-K, Tong K-L, Li Z (2005) Organometallics 24:4079–4082
66. He Z, Wong W-Y, Yu X, Kwok H-S, Lin Z (2006) Inorg Chem 45:10922–10937
67. Zhou G-J, Wang X-Z, Wong W-Y, Yu X-M, Kwok H-S, Lin Z (2007) J Organomet Chem 692:3461–3473
68. Cho J-Y, Domercq B, Barlow S, Suponitsky KY, Li J, Timofeeva TV, Jones SC, Hayden LE, Kimyonok A, South CR, Weck M, Kippelen B, Marder SR (2007) Organometallics 26:4816–4829

69. Balzani V, Carassiti V (1968) J Phys Chem 72:383–388
70. Andrews LJ (1979) J Phys Chem 83:3203–3209
71. McMillin DR, Moore JJ (2002) Coord Chem Rev 229:113–121
72. Wong KM-C, Yam VW-W (2007) Coord Chem Rev 251:2477–2488
73. Lai S-W, Chan MC-W, Cheung T-C, Peng S-M, Che C-M (1999) Inorg Chem 38:4046–4055
74. Lu W, Mi B-X, Chan MCW, Hui Z, Che C-M, Zhu N, Lee S-T (2004) J Am Chem Soc 126:4958–4971
75. Wang A, Xiong F, Morlet-Savary F, Li S, Li Y, Fouassier J-P, Yang G (2008) J Photochem Photobiol A 194:230–237
76. Lanoë P-H, Fillaut J-L, Toupet L, Williams JAG, Le Bozec H, Guerchais V (2008) Chem Commun 4333–4335
77. McGuire R Jr, Wilson MH, Nash JJ, Fanwick PE, McMillin DR (2008) Inorg Chem 47:2946–2948
78. Kwok C-C, Ngai HMY, Chan S-C, Sham IHT, Che C-M, Zhu N (2005) Inorg Chem 44:4442–4444
79. Williams JAG, Beeby A, Davies ES, Weinstein JA, Wilson C (2003) Inorg Chem 42:8609–8611
80. Farley SJ, Rochester DL, Thompson AL, Howard JAK, Williams JAG (2005) Inorg Chem 44:9690–9703
81. Rochester DL, Develay S, Zalis S, Williams JAG (2009) Dalton Trans: 1728–1741
82. Fattori V, Williams JAG, Murphy L, Cocchi M, Kalinowski J (2008) Photonics Nanostruct Fundam Appl 6:225–230
83. Develay S, Blackburn O, Thompson AL, Williams JAG (2008) Inorg Chem 47:11129–11142
84. Cocchi M, Kalinowski J, Virgili D, Fattori V, Develay S, Williams JAG (2007) Appl Phys Lett 90:023506
85. Kalinowski J, Cocchi M, Virgili D, Fattori V, Williams JAG (2007) Adv Mater 19:4000–4005
86. Virgili D, Cocchi M, Fattori V, Sabatini C, Kalinowski J, Williams JAG (2006) Chem Phys Lett 433:145–149
87. Kalinowski J, Cocchi M, Virgili D, Fattori V, Williams JAG (2007) Chem Phys Lett 447:279–283
88. Evans RC, Douglas P, Williams JAG, Rochester DL (2006) J Fluorescence 16:201–206
89. Botchway SW, Charnley M, Haycock JW, Parker AW, Rochester DL, Weinstein JA, Williams JAG (2008) Proc Natl Acad Sci U S A 105:16071–16076
90. Kozhevnikov VN, Donnio B, Bruce DW (2008) Angew Chem Int Ed 47:1–5